

AD-A214 796

1

REPORT DOCUMENTATION PAGE			Form Approved OMB No. 0704-0188	
Public reporting burden for this collection of information is estimated to average 1 hour per response, including the time for reviewing instructions, searching existing data sources, gathering and maintaining the data needed, and completing and reviewing the collection of information. Send comments regarding this burden estimate or any other aspect of this collection of information, including suggestions for reducing this burden, to Washington Headquarters Services, Directorate for Information Operations and Reports, 1215 Jefferson Davis Highway, Suite 1204, Arlington, VA 22202-4302, and to the Office of Management and Budget, Paperwork Reduction Project (0704-0188), Washington, DC 20503				
1. AGENCY USE ONLY (Leave blank)	2. REPORT DATE 15 Feb 1979	3. REPORT TYPE AND DATES COVERED Interim		
4. TITLE AND SUBTITLE A STUDY OF SOME ELECTROMAGNETIC PROBLEMS RELATING TO EMP TECHNOLOGY		5. FUNDING NUMBERS 61102F 2301/A3		
6. AUTHOR(S) Chen-To Tai		7. PERFORMING ORGANIZATION NAME(S) AND ADDRESS(ES) Department of Electrical & Computer Engineering University of Michigan Ann Arbor, MI 48109		
8. PERFORMING ORGANIZATION REPORT NUMBER A 79-1363		9. SPONSORING/MONITORING AGENCY NAME(S) AND ADDRESS(ES) AFOSR BLDG 410 BAFB DC 20332-6448		
10. SPONSORING/MONITORING AGENCY REPORT NUMBER AFOSR 77-3465		11. SUPPLEMENTARY NOTES		
12a. DISTRIBUTION/AVAILABILITY STATEMENT		12b. DISTRIBUTION CODE		
13. ABSTRACT (Maximum 200 words) For the equivalent circuit problem the development and the testing of a numerical technique for rational functions have been accomplished, A network modelling leading to a canonical ladder configuration was formulated. Finally the equivalent circuit representation of a thin biconical antenna is constructed based on these methods. The research shows that transfer functions involved in radiating and scattering problems can be represented by such an equivalent circuit representation. In contrast to the equivalent circuit representation suggested by C.E. Baum (Single Port Equivalent Circuits for Antenna and Scatterers, Interaction Note 295 Air Force Weapons Laboratory, March, 1979) the method does not require explicit knowledge of the poles these transfer functions.		<p style="text-align: center;">DTIC ELECTE NOV 29 1989 S B D</p>		
<p>DISTRIBUTION STATEMENT A</p> <p>Approved for public release; Distribution Unlimited</p>				
14. SUBJECT TERMS		15. NUMBER OF PAGES 67		
		16. PRICE CODE		
17. SECURITY CLASSIFICATION OF REPORT unclassified	18. SECURITY CLASSIFICATION OF THIS PAGE unclassified	19. SECURITY CLASSIFICATION OF ABSTRACT	20. LIMITATION OF ABSTRACT	

THE UNIVERSITY OF MICHIGAN
COLLEGE OF ENGINEERING
DEPARTMENT OF ELECTRICAL AND COMPUTER ENGINEERING
Radiation Laboratory

FINAL REPORT

Prepared for:

Air Force Office of Scientific Research
Bolling Air Force Base
Washington, D.C. 20332

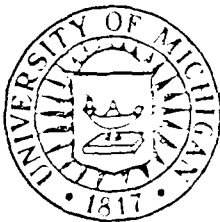
Grant No. 77-3465

30 September 1977 - 28 February 1979

Prepared by:

Professor Chen-To Tai
Project Director

15 February 1979



Ann Arbor, Michigan

A Study of Some Electromagnetic Problems
Relating to EMP Technology

This is the final report under Air Force Office of Scientific Research Grant No. 77-3465 bearing the above title covering the period from 30 September 1977 to 28 February 1979.

The research covers two main topics: the equivalent circuit representations of radiating systems and certain aspects of sensor characteristics. The detailed treatments have been written up and are attached as the appendices to this report. The following is a brief summary of the research results.

For the equivalent circuit problem the development and the testing of a numerical technique for rational functions have been accomplished. A network modelling leading to a canonical ladder configuration is then formulated. Finally the equivalent circuit representation of a thin biconical antenna is constructed based on these methods. The research shows that transfer functions involved in radiating and scattering problems can be represented by such an equivalent circuit representation. In contrast to the equivalent circuit representation suggested by C.E. Baum [Single Port Equivalent Circuits for Antenna and Scatterers, Interaction Note 295, Air Force Weapons Laboratory, March, 1975] our method does not require explicit knowledge of the poles of these transfer functions.

The second appendix treats the responses of a short dipole and a small loop placed in a right-angle conducting corner. The work is intended to correlate the open-circuit voltage of a sensor with the local surface charge density or surface current density on a scatterer. The right-angle corner is a simple structure for which an exact formulation of the problem can be given. The results show the exact relationship between the open circuit

voltage and the local surface charge or surface current density on the corner. The appendix also contains an investigation of the impedance functions of these probes taking into consideration the proximity effect of the corner.

The research on the equivalent circuit representation was presented at the Nuclear EMP Meeting held at the University of New Mexico, June 6-8, 1978. The paper is entitled "A Network Model for the Biconical Antenna," by C.B. Sharpe and C.J. Roussi. Our work on the sensor research has just been completed and will be submitted to the Air Force Weapons Laboratory for consideration of publication as a note in the Sensor Series.



Accession For	
NTIS GRA&I	<input checked="" type="checkbox"/>
DTIC TAB	<input type="checkbox"/>
Unannounced	<input type="checkbox"/>
Justification	
By _____	
Distribution/	
Availability Codes	
Dist	Avail and/or
	Special
A-1	

APPENDIX A

Equivalent Circuit Representation of
Radiation Systems

by

C. B. Sharpe and C. J. Roussi

Radiation Laboratory
Department of Electrical and Computer Engineering
The University of Michigan
Ann Arbor, Michigan

December, 1978

Abstract

In this report the biconical antenna is treated as a representative scattering system. It is shown that at its input terminals the biconical antenna can be modeled by a transmission line terminated in a canonical LC ladder network. The real and imaginary parts of the input impedance of the biconical antenna serve as useful test functions for studying the approximation of complex functions of frequency by rational functions. An effective algorithm for this purpose was implemented and evaluated. It is also shown that over a limited domain in the complex frequency plane the poles and zeros of the system function can be recovered via the rational approximation.

Table of Contents

Section	Page No.
1. Introduction.....	1
2. A Network Model for the Biconical Antenna..	1
3. Approximation by Rational Functions.....	5
4. References.....	9

1. Introduction

In developing equivalent circuits for radiating systems we have divided the problem into two basic parts: the development of a rational function approximation technique and the development of lumped network synthesis procedures appropriate to the system in question. Of course, the first part must serve as a basis for the second. Typically the rational function will represent in analytic form the transfer admittance of a system obtained by experimentally measuring the amplitude and phase of the surface current as a function of frequency at some point on the scattering object with reference to the incident electric field at some reference plane. In the general case all we can say about the transfer function is that its poles must all lie in the closed left half-plane. The zeros may lie in either half-plane. Among the parameters in the problem are the polarization and aspect of the incident field, the location and orientation of the current probe on the object and, of course, the shape of the scattering body. An important question which remains to be answered is the nature of the dependence of the poles and zeros of the transfer function on these parameters.

In order to explore the above question, much of our initial effort has been devoted to the development and testing of a numerical approximation technique for rational functions. This technique and its application in several representative approximation problems is described in Section 3. As a preliminary exercise, a network modelling problem leading to a canonical ladder configuration was also investigated and completed. This work is presented in the next section. Both of the above studies were centered around the biconical antenna. One reason for this approach is that the input impedance of the biconical antenna exhibits many of the frequency response characteristics of more general scattering structures, and is, therefore, a useful vehicle for test purposes.

2. A Network Model for the Biconical Antenna

The biconical antenna offers an interesting example on which to test network modeling techniques because an exact analytical expression for the input impedance is available. Tai^[1] has shown that the input impedance at the center of the biconical antenna can be represented by a section of uniform line terminated in a frequency-dependent admittance $Y_t(\omega)$. This equivalent circuit is illustrated in Figure 1, where

K denotes the characteristic impedance of the line. The following expression was obtained by Tai for Y_t :

$$Y_t = \frac{Z_0}{4\pi K^2} \left\{ 2L(2\beta z) + e^{2i\beta z} [L(2\beta z) - L(4\beta z) + \ln 2] + e^{-2i\beta z} [L^*(2\beta z) - \ln 2] \right\}, \quad (1)$$

where

$$L(x) = \int_0^x \frac{1 - \cos t}{t} dt + i \int_0^x \frac{\sin t}{t} dt$$

and the asterisk denotes the complex conjugate. The real and imaginary parts of $Y_t(\beta z)$ are plotted in Figure [2] for the case where the angle of the cone, $\theta_0 = .01$ radians.

The objective of the work described in this section is to construct a lumped network model for the load admittance Y_t of the equivalent circuit shown in Figure 1. Because Y_t represents a positive real driving point admittance, it is possible in principle to synthesize a network model from the real part of Y_t alone. From (1), the asymptotic behavior of the real part of $Y_t(\beta z)$ at low frequencies is given by

$$\lim_{\beta z \rightarrow 0} \text{Re}[Y_t(\beta z)] = \frac{Z_0}{6\pi K^2} (\beta z)^4,$$

where Z_0 is the characteristic impedance of free space. This suggests that we look for a network having an input admittance $Y_n(j\omega)$ such that

$$\text{Re}[Y_n(j\omega)] = \frac{\omega^4}{P(\omega^2)}, \quad (2)$$

where $P(\omega^2)$ is a polynomial of the form

$$P(\omega^2) = p_0 + p_2\omega^2 + \dots + p_{4n}\omega^{4n}.$$

It will now be shown that $Y_n(s)$ can always be realized as an LC ladder terminated in a resistance if $P(\omega^2) > 0$, all ω .

Suppose a lossless network is excited as shown in Figure [3] and assume that the scattering coefficient $S_{21}(s)$ has the form

$$S_{21}(s) = \frac{A(s)}{B(s)}, \quad (3)$$

where $B(s)$ is a polynomial of degree $2n$ having all its roots in the LHP. Then if $A(s)$ is another polynomial of degree $2n$, $S_{11}(s)$ will have the form

$$S_{11}(s) = \frac{A(s)}{B(s)} .$$

The unitary condition,

$$S_{11}(s)S_{11}(-s) + S_{21}(s)S_{21}(-s) = 1 ,$$

implies that

$$B(s)B(-s) - A(s)A(-s) = s^4 . \quad (4)$$

This is the only condition on $A(s)$. The input admittance can be expressed by

$$Y_n(s) = \frac{1 - S_{11}(s)}{1 + S_{11}(s)} = \frac{W(s)}{U(s)} ,$$

where $U(s) = A(s) + B(s)$ and $W(s) = B(s) - A(s)$. Equation (4) leads to the relation,

$$U(s)W(-s) + U(-s)W(s) = 2s^4 , \quad (5)$$

between $U(s)$ and $W(s)$. Using this result

$$\begin{aligned} \operatorname{Re}\{Y_n(j\omega)\} &= \frac{1}{2} \left(\frac{W(j\omega)}{U(j\omega)} + \frac{W(-j\omega)}{U(-j\omega)} \right) \\ &= \frac{4}{U(j\omega)U(-j\omega)} . \end{aligned}$$

Thus, the polynomial $P(\omega^2)$ can be identified with the product

$$P(\omega^2) = U(j\omega)U(-j\omega) .$$

Finally, it can be shown that the transmission function given in (3) can be realized by a ladder network of the form shown in Figure [4]. The number of independent energy storage elements, $2n$, corresponds to the number of poles of $S_{21}(s)$ and the two zeros of transmission required at $s = 0$ are provided by C_1 and L_1 . It should be noted that this realization of $S_{21}(s)$ is not unique.

The numerical aspect of the modeling problem involves the determination of the coefficients of $P(\omega^2)$ by curve-fitting the function $\omega^4/P(\omega^2)$ to the "data" represented by $\operatorname{Re}\{Y_t(\frac{j\omega}{c})\}$. This can most readily be done by forming the objective function

$$F = \sum_{i=1}^{N} W_i \left[\frac{\omega_i^4}{\operatorname{Re}\{Y_t(\frac{j\omega_i}{c})\}} - P(\omega_i^2) \right]^2 , \quad (6)$$

where the W_i are arbitrary weighting coefficients. In the results that follow $W_i = 1$, all i , and the normalization $\omega=c$ was employed. The optimum

frequency range over which the data function was sampled is a function of n and was determined empirically.

Of course the advantage of employing a least-squares objective function as defined in (5) is that the minimization of F with respect to the p_i , $i=0, 2, \dots, 4n$, leads to a system of linear equations for the unknown coefficients. The algorithm is easily implemented and the solution for the coefficients presents no difficulty as long as the corresponding matrix remains well-conditioned. Chebyshev polynomial methods or near minimax approximations such as Lawson's algorithm [2], can be used to avoid the ill-conditioning that frequently occurs for large values of n , although we did not find this to be necessary. Once the polynomial $P(s^2)$ is known $U(s)$ can be recovered from

$$P(-s^2) = U(s)U(-s)$$

by factorization if $P(s^2) > 0$, all s . Thus, $U(s)$ contains the LHP roots of $P(-s^2)$.

Suppose $U(s)$ has the form

$$U(s) = d_0 + d_1s + \dots + d_{2n}s^{2n}.$$

Then $W(s)$ will have the form

$$W(s) = c_1s + c_2s^2 + \dots + c_{2n-1}s^{2n-1}.$$

The latter polynomial can be determined uniquely from $U(s)$ by imposing the condition given in (5). For instance, in the case of $n=3$, the equations for the c_i take the form,

$$\begin{bmatrix} 0 & 0 & 0 & d_6 & -d_5 \\ 0 & d_6 & -d_5 & d_4 & -d_3 \\ -d_5 & d_4 & -d_3 & d_2 & -d_1 \\ -d_3 & d_2 & -d_1 & d_0 & 0 \\ -d_1 & d_0 & 0 & 0 & 0 \end{bmatrix} \begin{bmatrix} c_1 \\ c_2 \\ c_3 \\ c_4 \\ c_5 \end{bmatrix} = \begin{bmatrix} 0 \\ 0 \\ 0 \\ 1 \\ 0 \end{bmatrix}$$

The synthesis procedure is completed by expanding $Y_n(s) = W(s)/U(s)$ in a continued fraction and identifying the coefficients with the elements of the ladder network. Thus, for the network of Figure 4, the expansion takes the form,

$$Y_n(s) = \frac{1}{\frac{1}{sC_1} + \frac{1}{\frac{1}{sL_1} + \frac{1}{sL_2 + \frac{1}{sC_2 + \dots + \frac{1}{sC_n + \frac{1}{R}}}}}}$$

Figures 5 and 6 illustrate some typical results obtained by the modeling technique described above. In each case $\theta_0 = .01$ radians. The element values for the approximating network are calculated assuming $\beta = \text{lm}$. It can be seen that the least-squares fit in the real part of the admittance is quite satisfactory and that the band over which the approximation is valid increases, as expected, with the order of the network. It can be seen from Figures 7 and 8 that the approximation in the real and imaginary parts of Z_{in} , the input impedance of the antenna, is not as good as that obtained for Y_t . This can be explained by noting that the error in approximating $\text{Im}[Y_t]$ is not controlled in the present procedure and, therefore, it contributes to the observed error in Z_{in} when transferred through the transmission line. To avoid this effect, it would be necessary to control both the real and imaginary parts of Y_n . This could be accomplished by using the ladder element values obtained here as initial values in a computer-aided design procedure. In this event a nonlinear function minimization algorithm would be required.

In conclusion, it has been shown that the biconical antenna can be effectively modeled by a transmission line terminated in an LC ladder network with a resistive load. It has been shown that the modeling problem can be reduced to a straightforward numerical approximation procedure followed by a direct synthesis algorithm.

3. Approximation by Rational Functions

3.1 Theory

It is often the case that one would like to express the transfer function of a linear system as the ratio of two polynomials. This form is preferred as it lends itself to linear transform methods of solution. Of the techniques that have been developed to fit experimental data by such rational functions [3]-[4], the one by Levy is the most notable [5]-[6] and forms the basis of the rational approximation method examined in this report.

A function of the form

$$H(j\omega) = \frac{a_0 + a_1(j\omega) + \dots + a_n(j\omega)^n}{b_0 + b_1(j\omega) + \dots + b_m(j\omega)^m} = \frac{N(j\omega)}{D(j\omega)}$$

is chosen to approximate (in the least-squares sense) a given complex set of data $F_i = F_{Ri} + jF_{Ii}$, $i=1, \dots, N$, where $H(j\omega)$ represents, for example, the transfer function of a lumped network and F_i the steady-state data associated, for example, with the current at some point on a scattering object. The a_i and b_i coefficients are found by minimizing

$$E = \sum_{i=1}^N |F_i - H(j\omega_i)|^2 = \sum_{i=1}^N |e_i|^2.$$

The problem with this formulation is two-fold: E is a nonlinear function of the unknown coefficients and the low frequency data is not weighted sufficiently. As a result, wide swings in the input data will cause large approximating errors at low frequencies. These problems may be remedied by defining a new error,

$$e_i^* = \frac{D^k(j\omega)}{D^{k-1}(j\omega)} e_i,$$

where the superscript k refers to the iteration number. If, after each iteration, one refines the error estimate in this way and minimizes again, a much better approximation is obtained. Sanathanan and Koerner [7] have shown that $D^k \approx D^{k-1}$ after a sufficient number of linear iterations. With this change, the object function now becomes

$$E^* = \sum_{i=1}^N \left| \frac{[D_R(j\omega_i) + jD_I(\omega_i)][F_R(j\omega_i) + jF_I(\omega_i)] - [N_R(j\omega_i) + jN_I(\omega_i)]}{D^{k-1}(j\omega_i)} \right|^2$$

$$= \sum_{i=1}^N \left| [D_R + jD_I][F_R + jF_I] - [N_R + jN_I] \right|^2 W_{ik},$$

where $W_{ik} = \frac{1}{|D^{k-1}|^2}$ is a weight function, and the subscripts R and I indicate the real and imaginary parts of the terms. The minimization of E^* at each iteration is now a linear problem. To this end E^* is partially differentiated with respect to each of the polynomial coefficients and equated to zero. This yields the following matrix equation:

The minimization of E^* at each iteration is now a linear problem. To this end E^* is partially differentiated with respect to each of the polynomial coefficients and equated to zero. This yields the following matrix equation:

$$\begin{bmatrix}
 \lambda_0 & 0 & -\lambda_2 & 0 & \lambda_4 & \dots & T_1 & S_2 & -T_3 & S_4 & \dots \\
 0 & \lambda_2 & 0 & -\lambda_4 & 0 & \dots & -S_2 & T_3 & S_4 & -T_5 & \dots \\
 \lambda_2 & 0 & -\lambda_4 & 0 & \lambda_6 & \dots & T_3 & S_4 & -T_5 & S_6 & \dots \\
 0 & \lambda_4 & 0 & -\lambda_6 & 0 & \dots & -S_4 & T_5 & S_6 & -T_7 & \dots \\
 \vdots & \vdots \\
 T_1 & -S_2 & -T_3 & S_4 & T_5 & \dots & U_2 & 0 & -U_4 & 0 & \dots \\
 S_2 & T_3 & -S_4 & -T_5 & S_6 & \dots & 0 & U_4 & 0 & -U_6 & \dots \\
 T_3 & -S_4 & -T_5 & S_6 & -T_7 & \dots & U_4 & 0 & -U_6 & 0 & \dots \\
 S_4 & T_5 & -S_6 & -T_7 & S_8 & \dots & 0 & U_6 & 0 & -U_8 & \dots \\
 \vdots & \vdots
 \end{bmatrix}
 \begin{bmatrix}
 a_0 \\
 a_1 \\
 \vdots \\
 \vdots \\
 b_0 \\
 b_1 \\
 \vdots \\
 \vdots
 \end{bmatrix}
 =
 \begin{bmatrix}
 S_0 \\
 T_1 \\
 S_2 \\
 T_3 \\
 \vdots \\
 0 \\
 U_2 \\
 0 \\
 U_4 \\
 \vdots
 \end{bmatrix}$$

where

$$\lambda_i = \sum_{k=1}^n w_k^i W_{kL}$$

$$S_i = \sum_{k=1}^n w_k^i R_k W_{kL}$$

$$T_i = \sum_{k=1}^n w_k^i I_k W_{kL}$$

$$U_i = \sum_{k=1}^n w_k^i (R_k^2 + I_k^2) W_{kL}$$

R_k and I_k are the real and imaginary parts of the transfer function at experimental points, and L is the iteration number. The coefficients b_1, b_2, \dots evaluated at the $L-1$ iteration are used to refine the weighting function W_L for the next iteration.

A FORTRAN program has been written implementing the above complex-curve fitting algorithm.

3.2 Applications

The aforementioned method was applied to the data generated by the terminating admittance function Y_t of the biconical-antenna model as given by Tai [1]. The data is shown in Figure 2. A rational function with eighth order numerator and ninth-order denominator was chosen to fit this data over a range of normalized frequency $0 \leq \beta l \leq 15$. This choice of transfer function was based upon the results of tests using the same program to fit the input impedance of an ideal transmission-line

terminated in a resistance. The results of the Y_t approximation are shown in Figure 9 and Figure 10.

Another test was performed on data describing the input impedance of the biconical antenna as shown in Figure 11. This example was approximated by a ninth-order numerator and tenth-order denominator. The results are presented in Figure 12 and Figure 13. It is seen by comparing these results with Figure 11 that the approximated imaginary part of Z_{in} fails to fit the data near $3\lambda=0$. This is due to a pole at zero which the data contained that the rational approximating function could not accommodate due to its chosen structure. This could have been corrected by changing the data and reinserting the pole later, a technique described by Levy [5].

The poles and zeros of the approximating function were extracted by standard techniques and compared with those found by Tai and Cho via a grid search. The result is shown in Figure 14. The poles and zeros reflect the closeness of the fit over the approximating range.

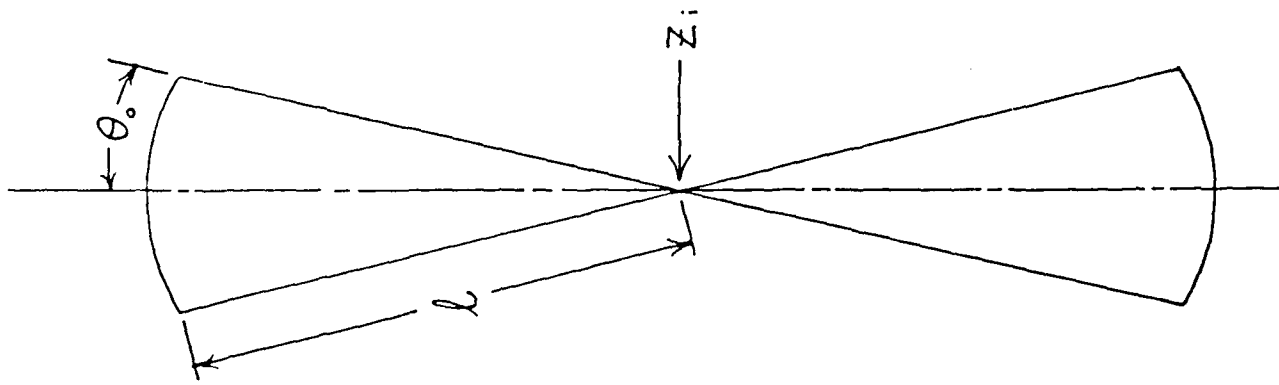
3.3 Conclusion

The rational function approximation method employed here has the advantage of being able to produce an analytic representation of data that is amenable to linear transform methods of solution. Furthermore, the implementation of the method is straightforward and computationally efficient. For the accuracy achieved here, the typical run took 2 CPU seconds (Amdahl 470) and cost \$.50.

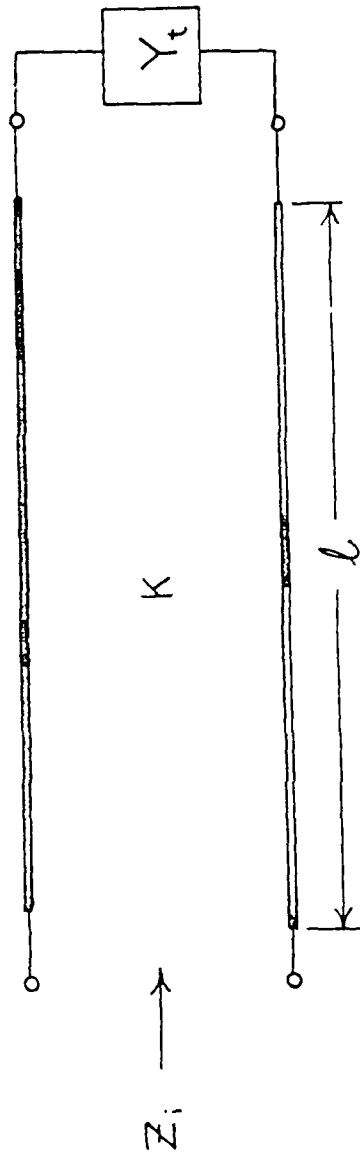
As a final remark, a more nearly mini-max approximation could be obtained by incorporating Lawson's algorithm [2] in the iterative procedure but our investigations to date do not indicate that this will be necessary.

References

- [1] C. T. Tai, "The Theory of Linear Antennas", Chapter 8, R.W.P. King, Harvard University Press, Cambridge, Mass. (1956).
- [2] C. L. Lawson, "Contributions to the Theory of Linear Least Maximum Approximations", Doctoral Thesis, University of California, Los Angeles (1961).
- [3] A. A. Kandshaw and L. V. Kanyushin, "Determining System Parameters From Experimental Frequency Characteristics", Automation and Remote Control, Vol. 19, No. 4, pp. 327, 1958.
- [4] G. L. Raskin, B. A. Mitsofanov, Y. O. Shtenerberg, "On the Determination of Numerical Values of the Coefficients of the Transfer Function of Linearized Links and Systems from Experimental Frequency Characteristics", Automation and Remote Control, Vol. 16, No. 5, 1955.
- [5] E. C. Levy, "Complex Curve Fitting", IRE Trans. on Automatic Control, Vol. AC-4, pp. 37-44, May 1959.
- [6] A. I. Petrenko, V. P. Sigorsky, "Algorithmic Analysis of Electronic Circuits", pp. 519-523.
- [7] C. K. Sanathanan and J. Koerner, IEEE Trans. on Auto. Cont., AC-8, January 1963, pp. 56-58.



BICONICAL ANTENNA



EQUIVALENT CIRCUIT FOR THE INPUT IMPEDANCE

$$K = \frac{Z_0}{\pi} \ln\left(\frac{2}{\theta_0}\right)$$

Figure 1.

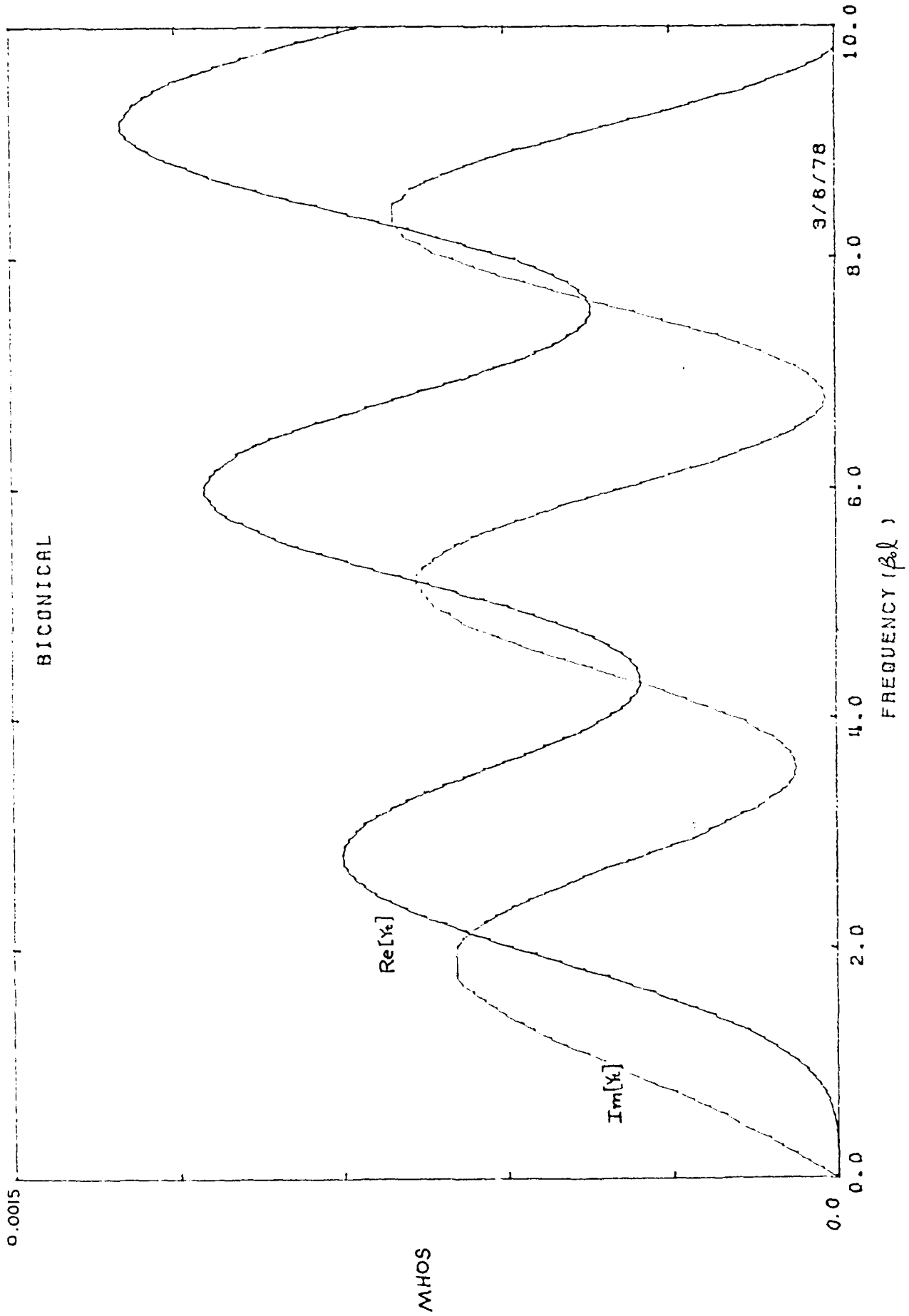


Figure 2

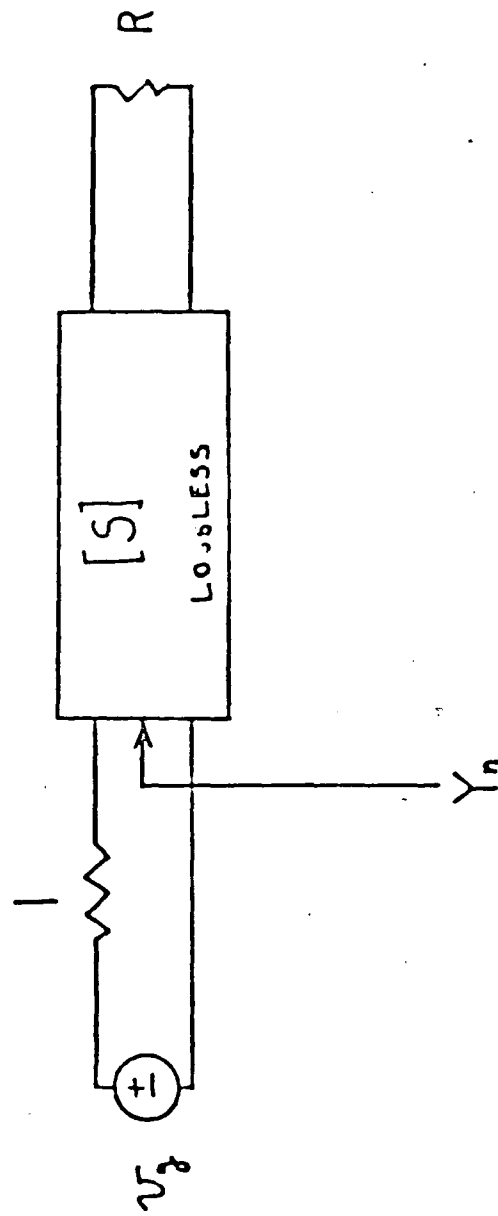
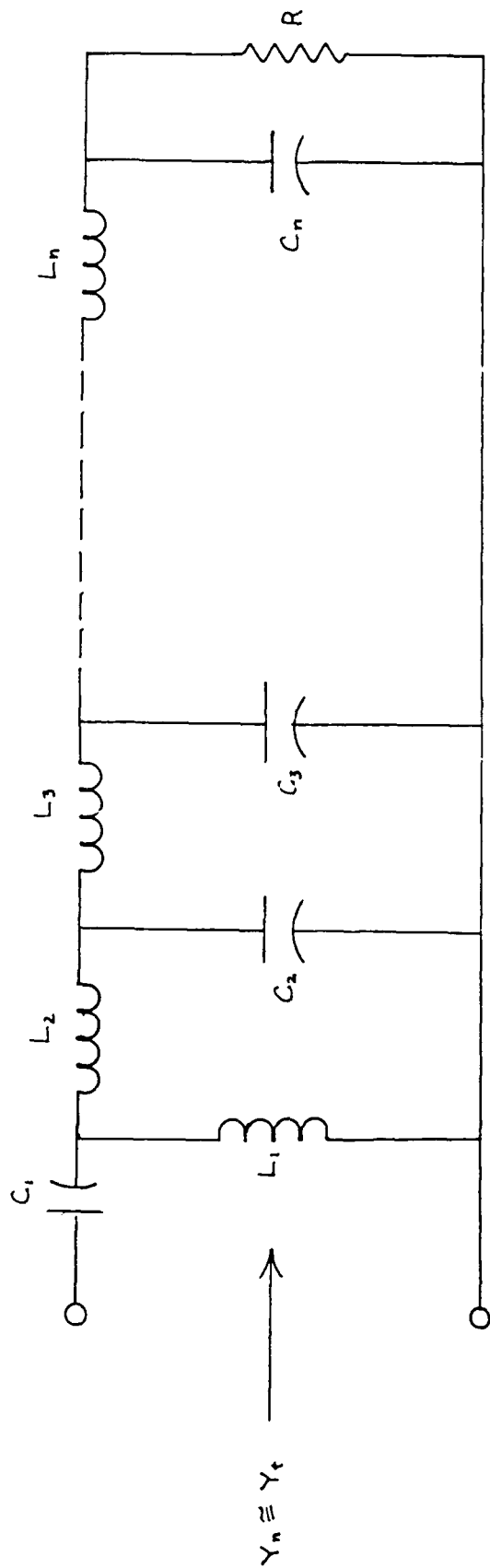
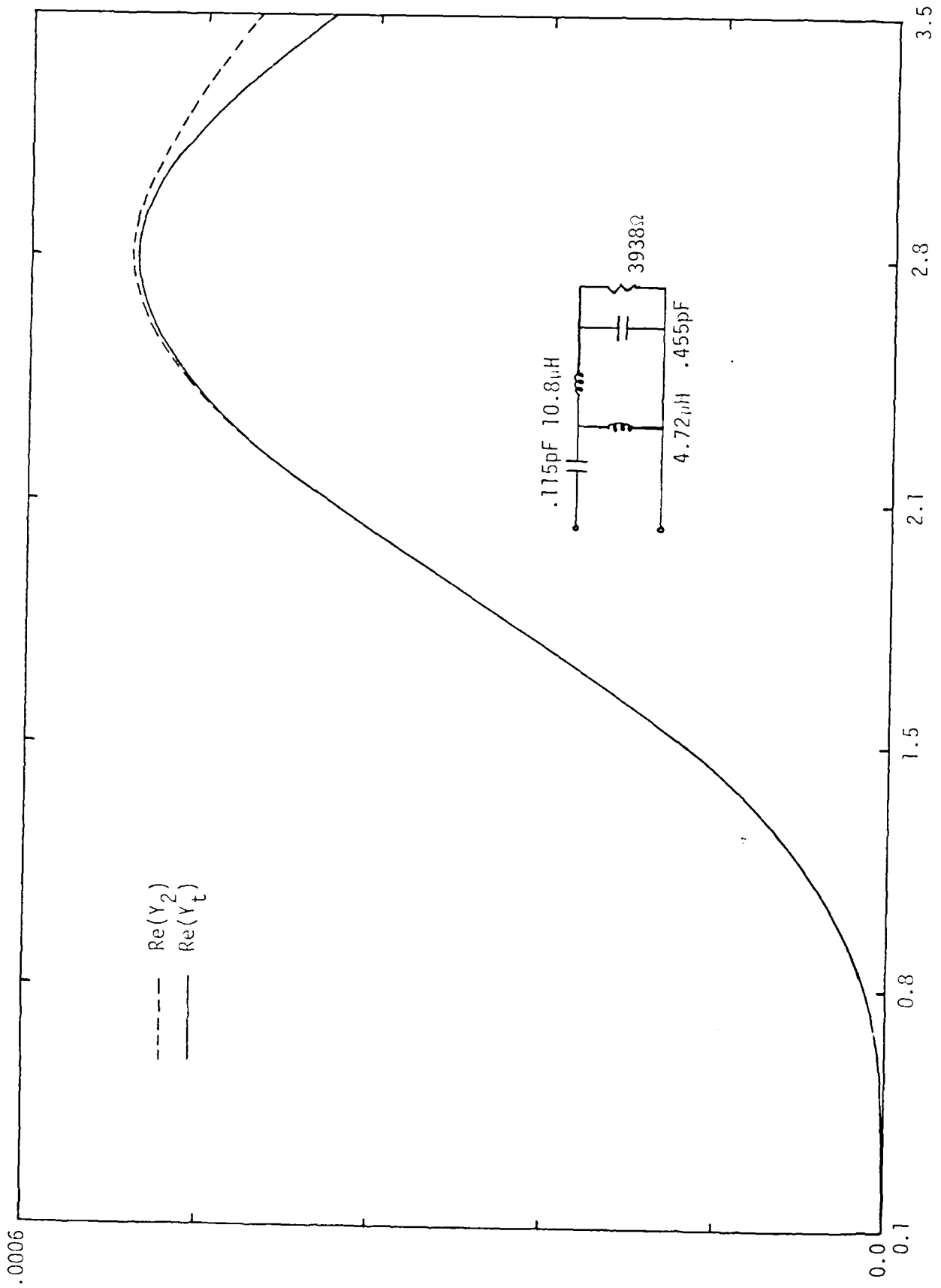


Figure 3

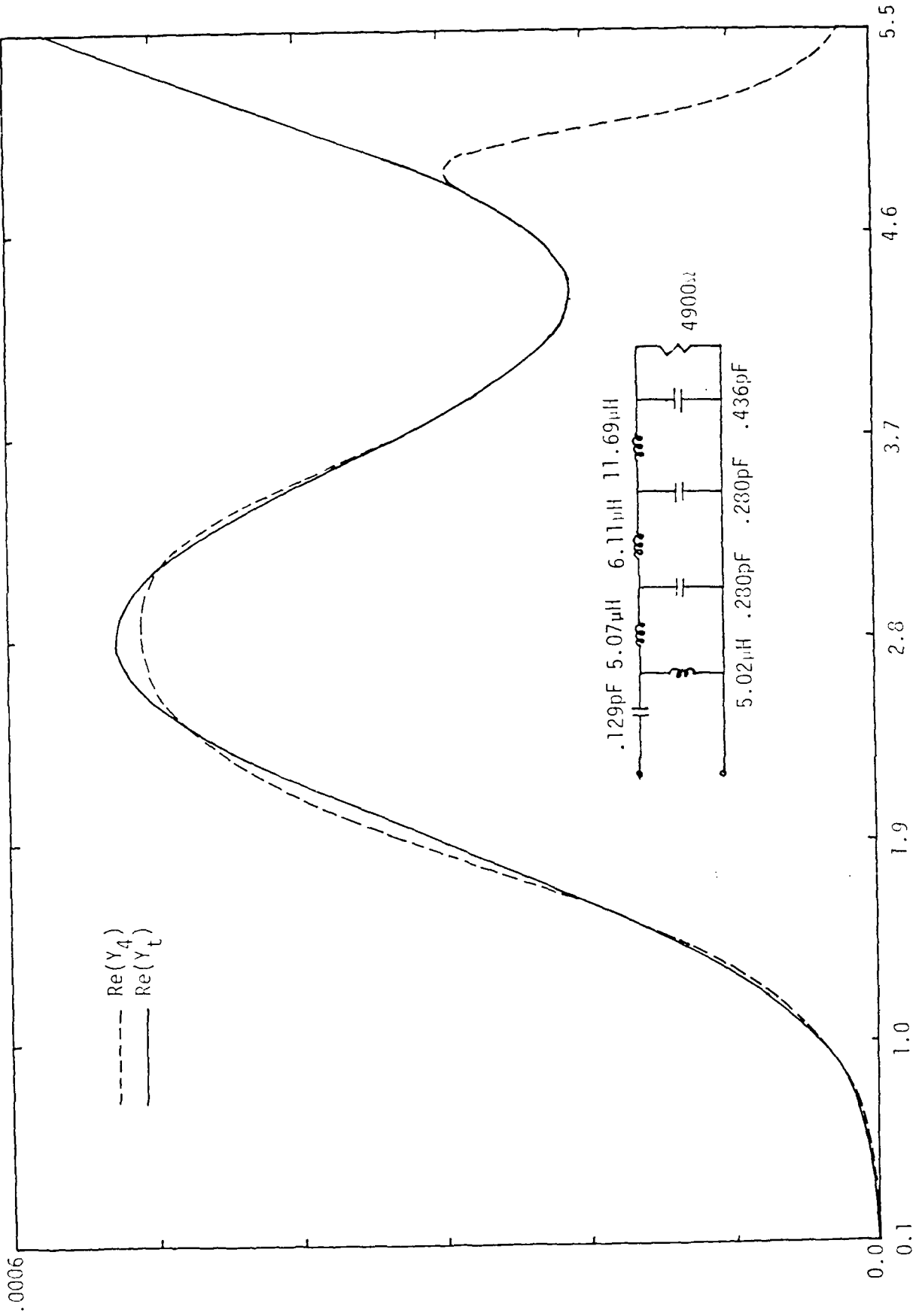


LOW-FREQUENCY LUMPED CIRCUIT MODEL FOR Y_e

Figure 4



βL
 Figure 5



MHz

Figure 6

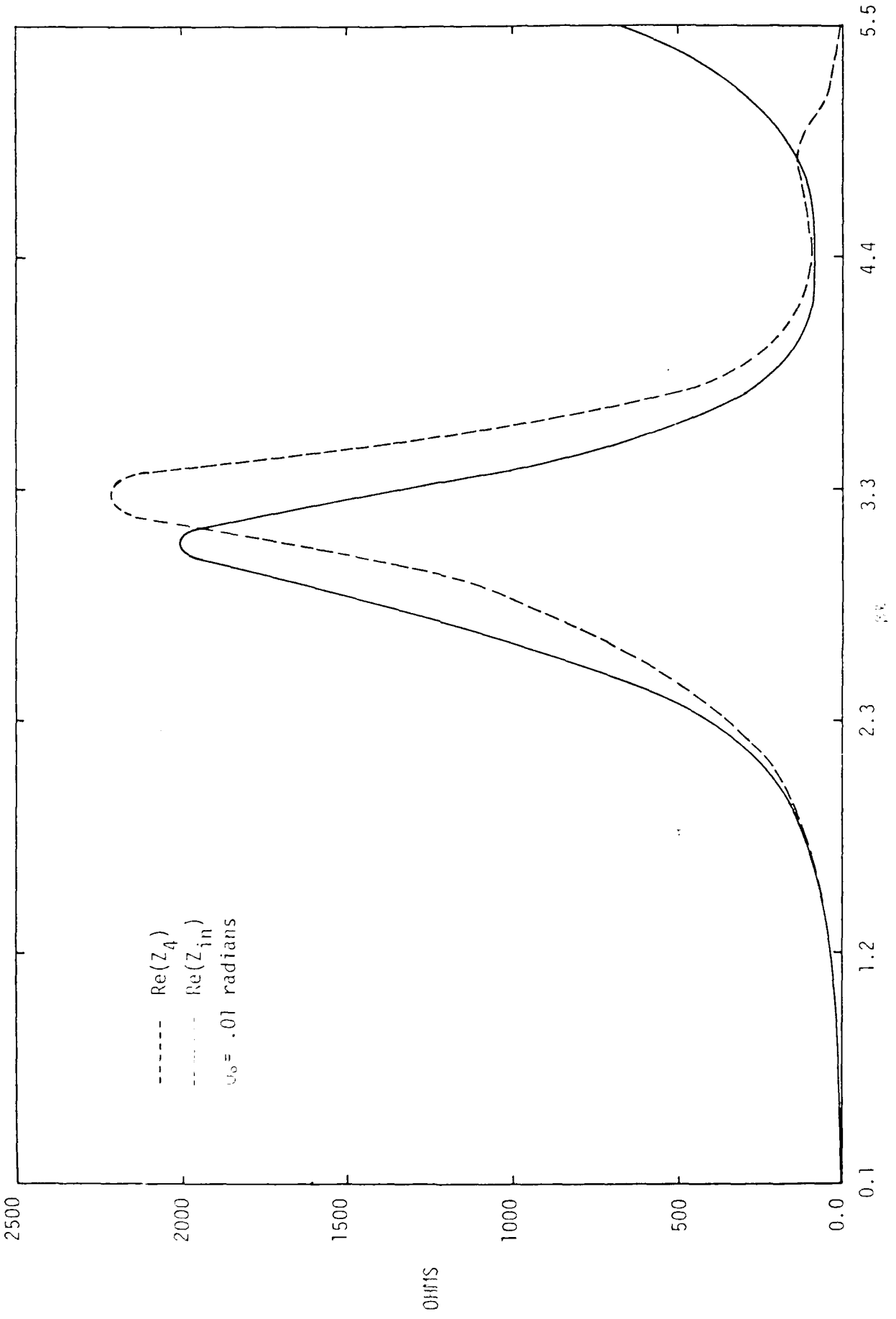


Figure 7

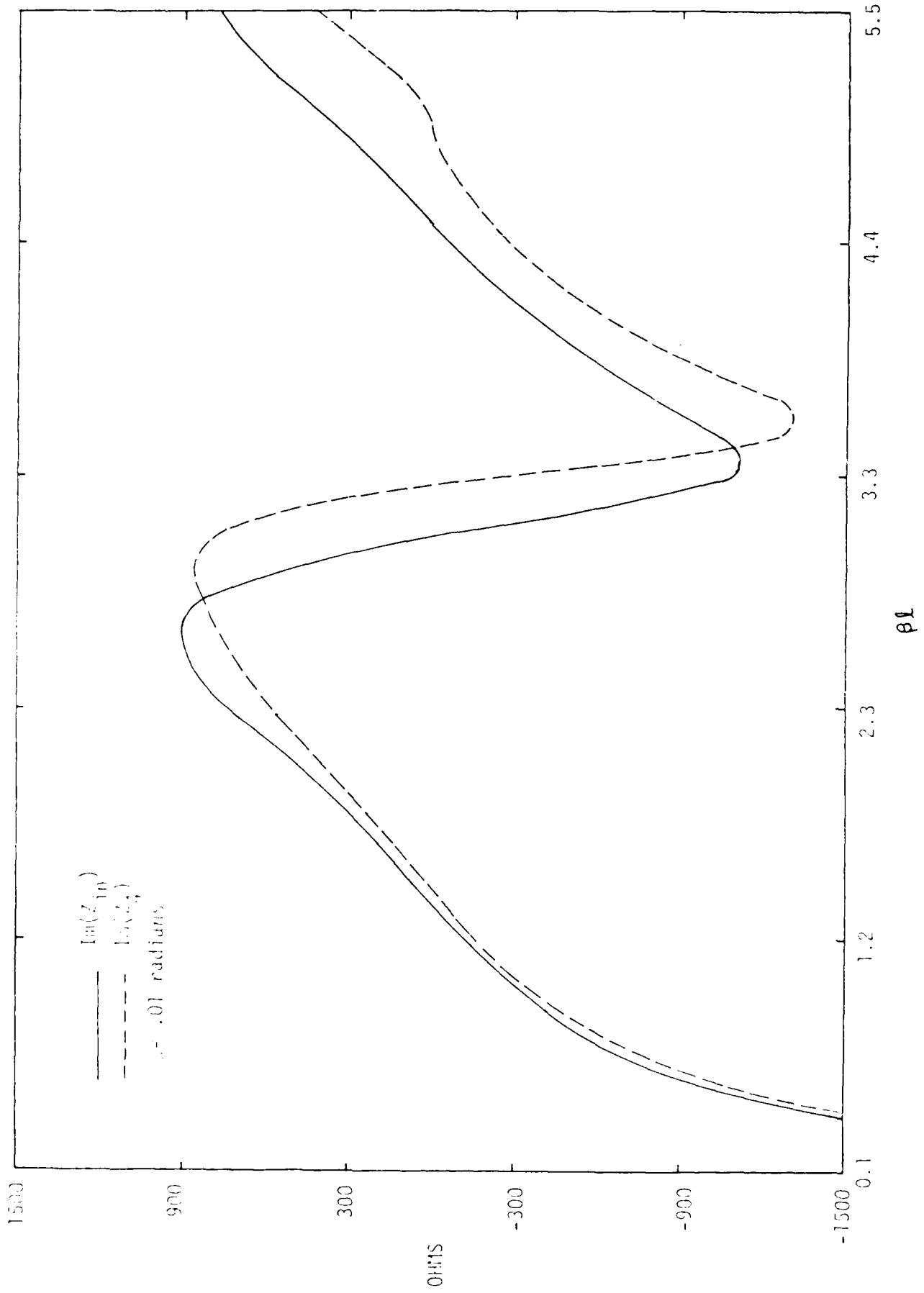


Figure 8

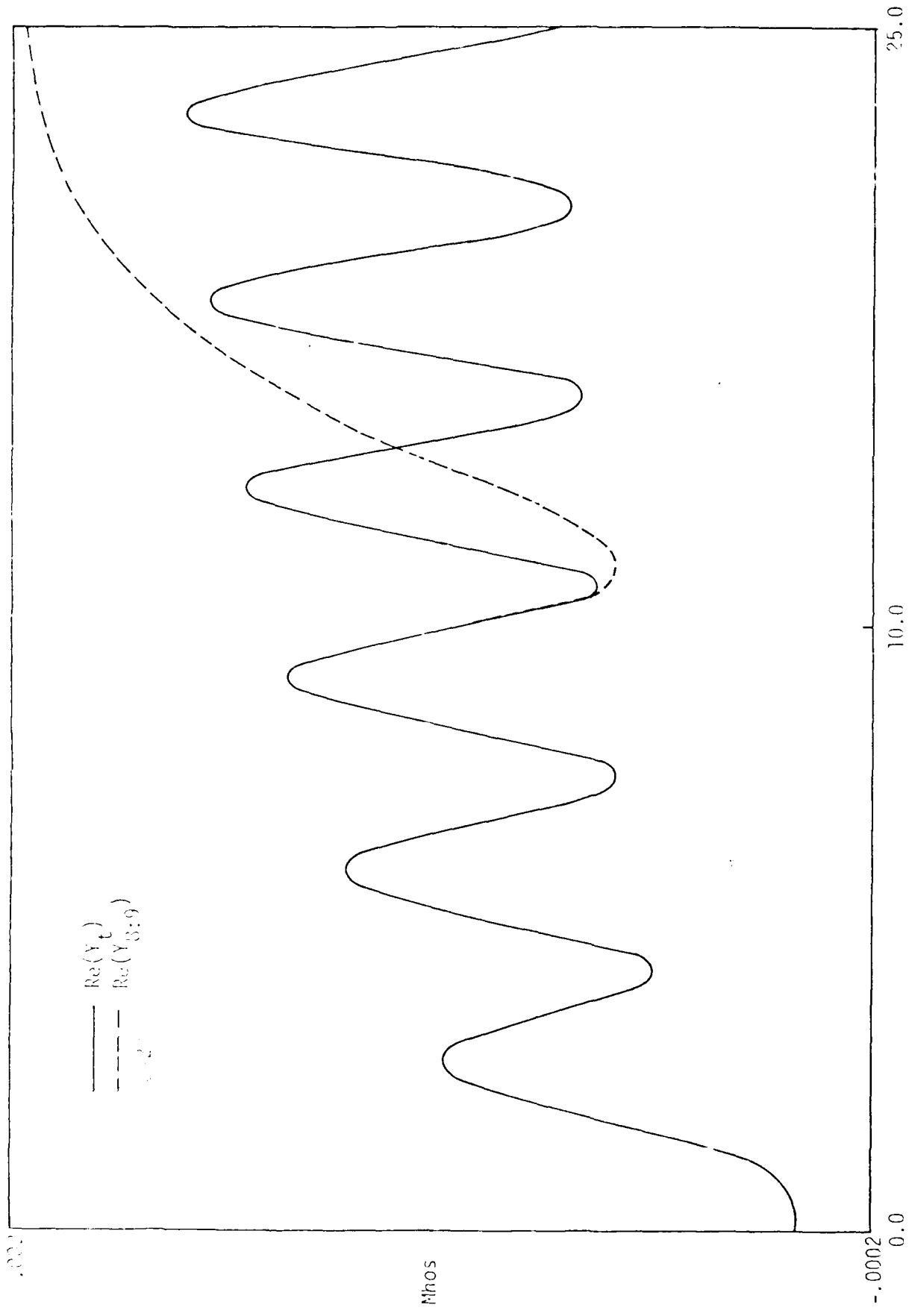


Figure 9

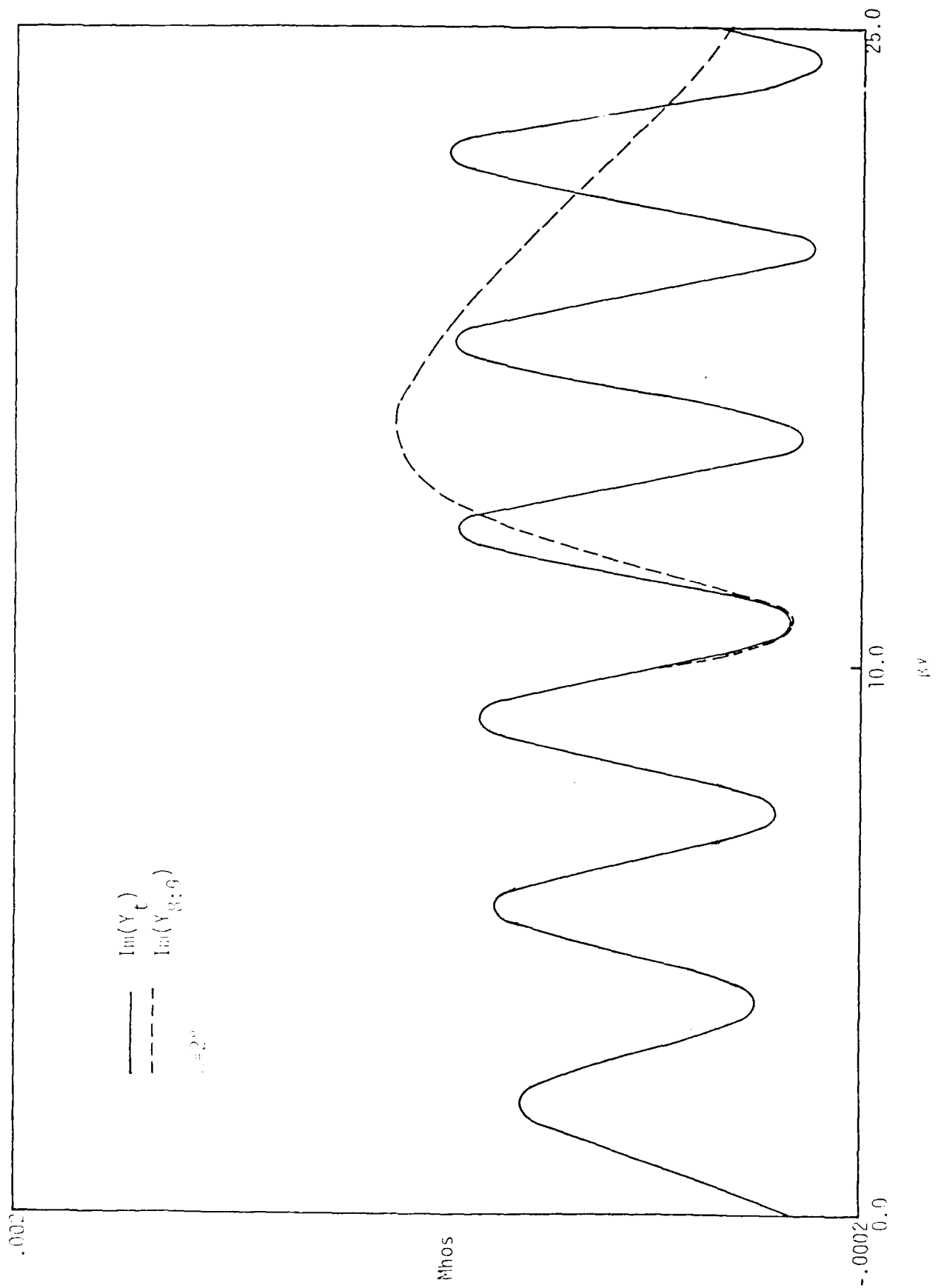


Figure 10

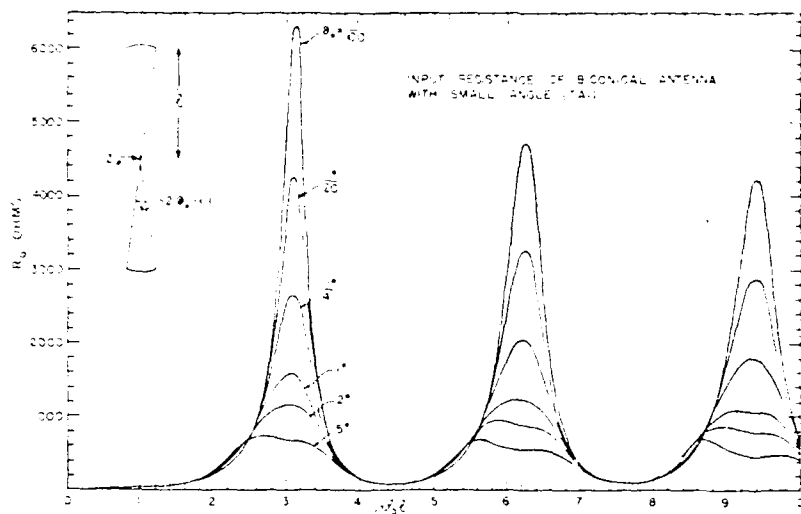


Fig. 10.3. Input resistance of biconical antenna with small angle (Tai).

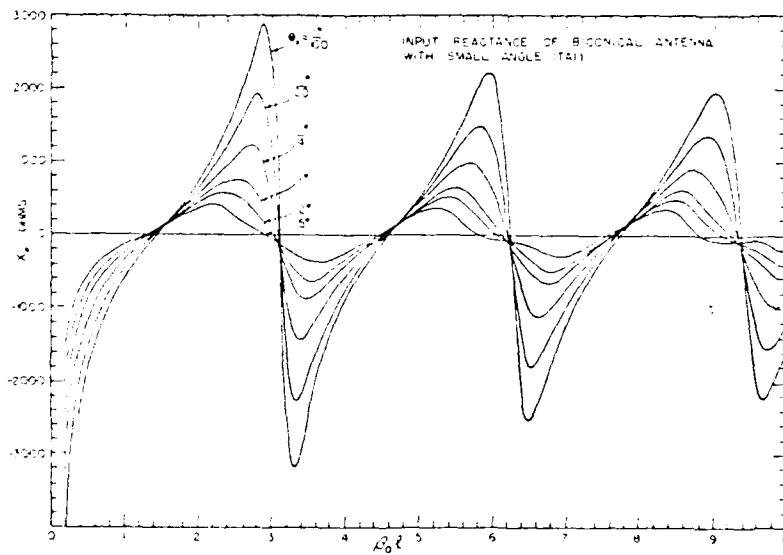


Fig. 10.4. Input reactance of biconical antenna with small angle (Tai).

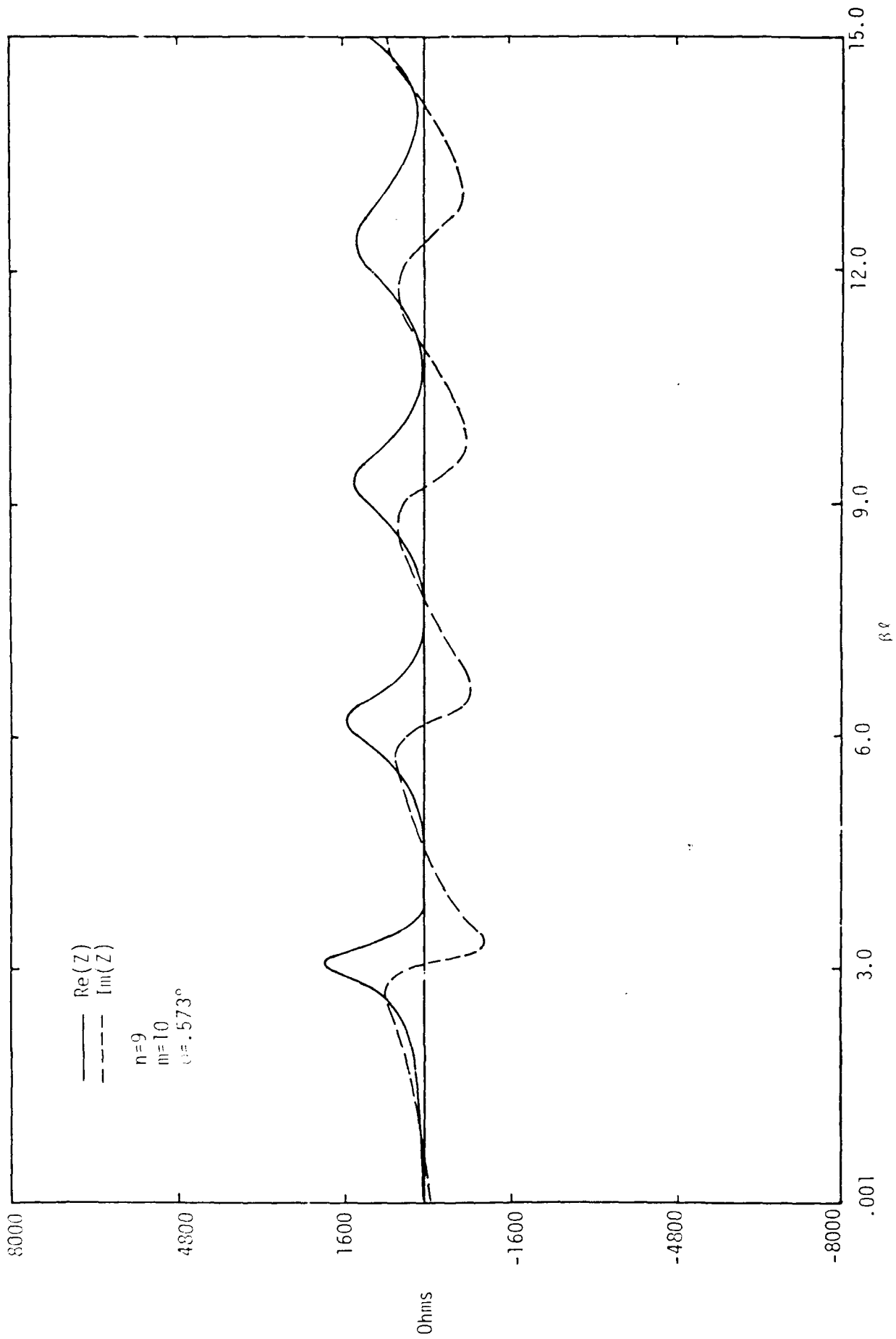


Figure 12

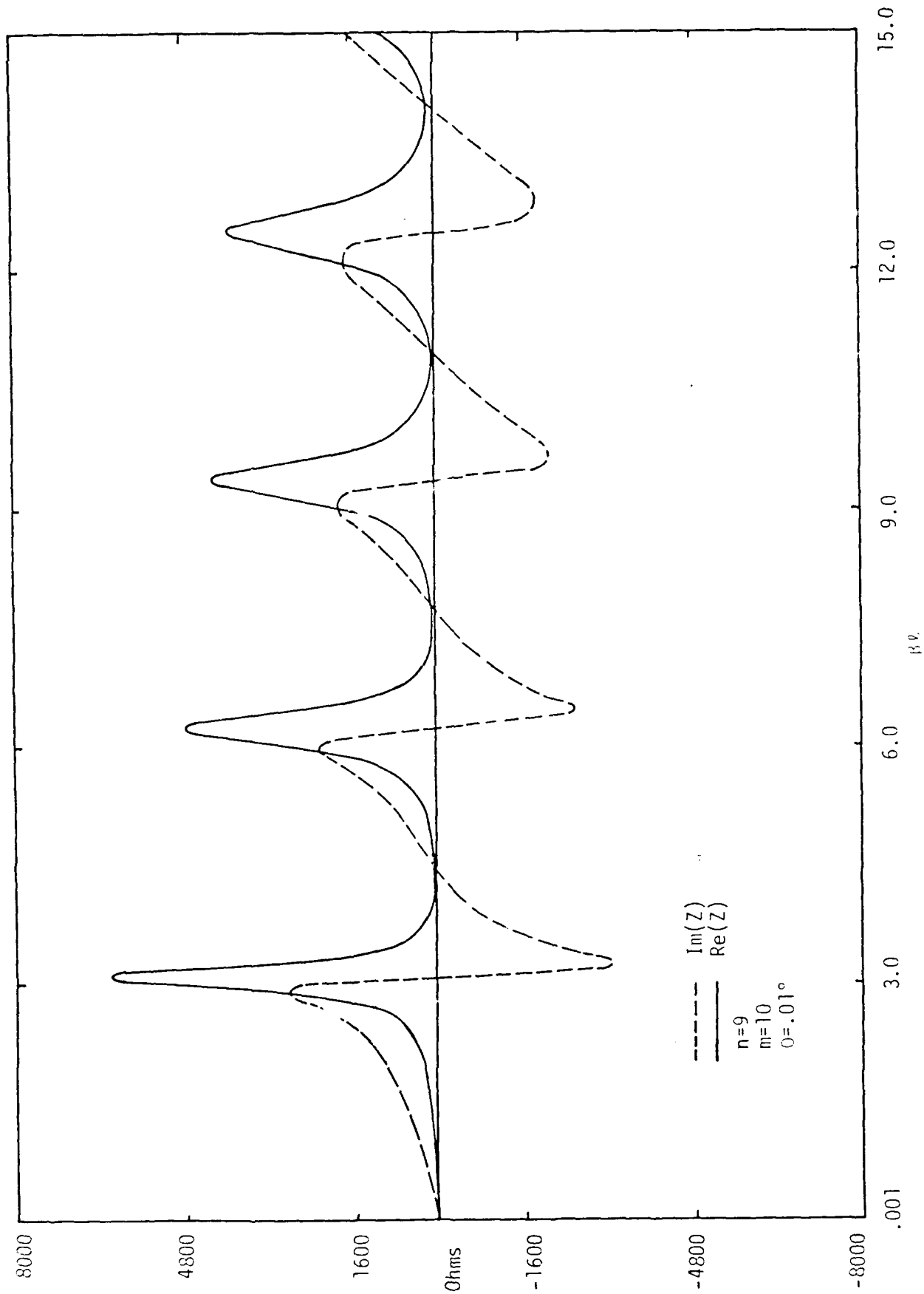


Figure 13

$$F(j\omega) = \frac{N^{(9)}}{D^{(10)}}$$

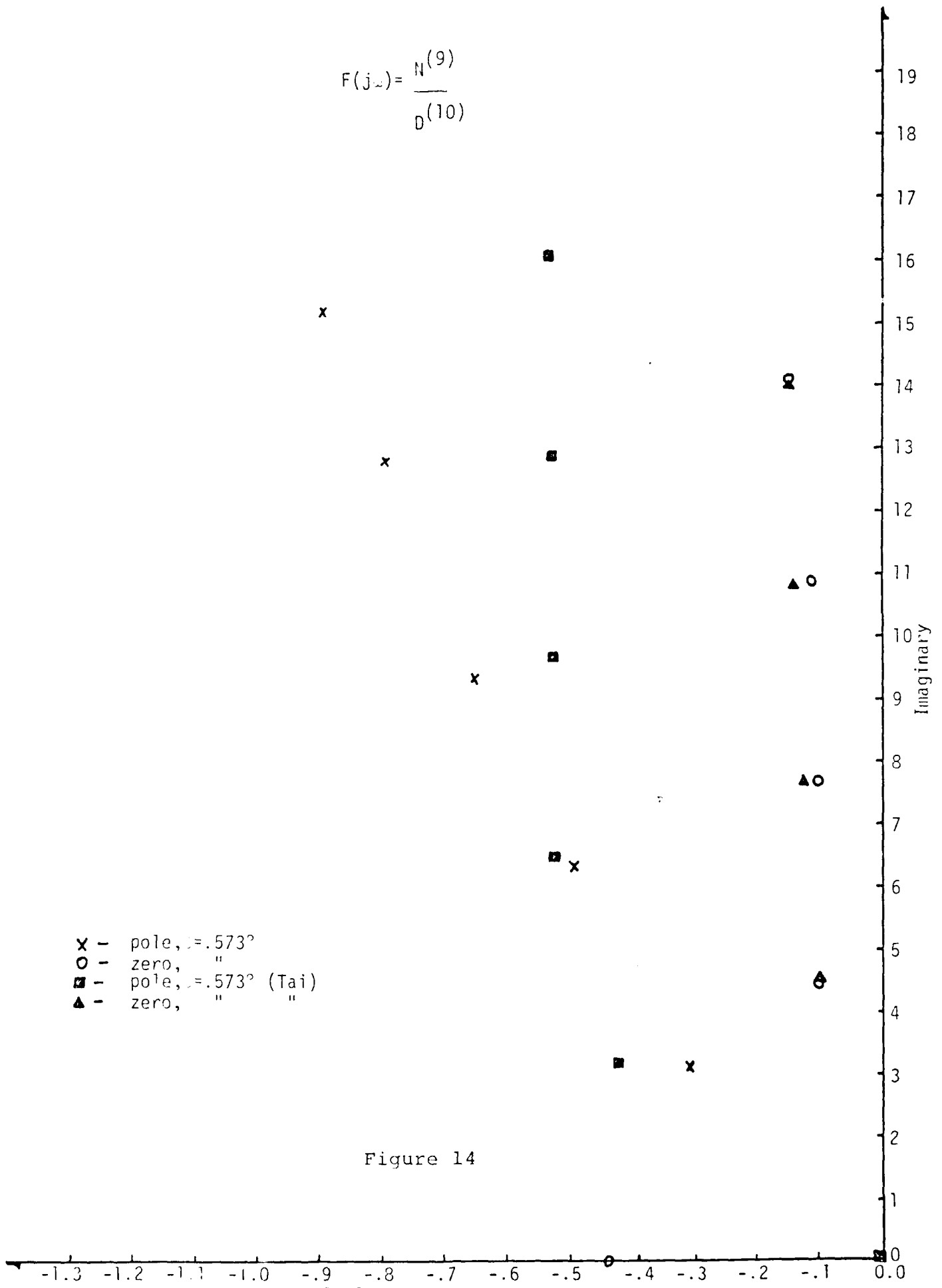


Figure 14

AN INVESTIGATION OF THE DETECTION OF THE SURFACE FIELDS OF
A RIGHT-ANGLE CORNER REFLECTOR BY SOME ELECTRICALLY SMALL SENSORS

by

Fariborz Jahanshahi

and

Chen-To Tai

The Radiation Laboratory
The Department of Electrical and Computer Engineering
The University of Michigan
Ann Arbor, Michigan 48109

November 1978

ABSTRACT

This report deals with the surface fields or the surface charge and current densities on a right-angle corner reflector induced by a polarized uniform plane wave. Equivalent circuit parameters of a short monopole and a small semi-loop mounted on the wedge are derived and explicit correlations between measurable quantities and local surface fields are established.

TABLE OF CONTENTS

<u>Section</u>	<u>Page</u>
1. INTRODUCTION	1
2. INDUCED SURFACE CURRENT AND CHARGE DENSITIES ON A RIGHT-ANGLE CORNER REFLECTOR BY A PLANE WAVE	2
3. OPEN CIRCUIT VOLTAGE OF A SHORT MONOPOLE AND A SMALL SEMI-LOOP MOUNTED ON THE REFLECTOR	5
4. INPUT IMPEDANCE OF THE PROBES	9
5. CORRELATION OF THE UNPERTURBED SURFACE FIELDS TO THE EQUIVALENT CIRCUIT PARAMETERS	31
6. REFERENCES	34

1. INTRODUCTION

The class of problems related to the measurements of the electromagnetic field quantities have attracted the attention of many engineers engaged in sensor research. The major difficulty encountered in the measuring process of any energy related physical quantity is the interaction of the measuring device(s) with the physical field that always produces a perturbation of the field. Therefore it is essential to have an a priori estimate on the amount of the extracted energy by the sensor and the extent of the perturbation. In this report we will consider a canonical problem of this class, namely the problem of measurement of surface fields on a right-angle corner reflector. A good account of the previous work on closely related problems is given in [2].

The geometry of the problem is shown in Figure 1.1. The walls of the wedge are perfectly conducting and the medium of propagation of the waves is air with parameters $(\epsilon, \mu, \sigma = 0)$. We will assume that the illuminating polarized uniform plane wave is propagating in a plane normal to the axis of the wedge. Furthermore only linearly polarized waves will be considered with polarization of the \vec{E} -field perpendicular and parallel to the axis of the wedge respectively.

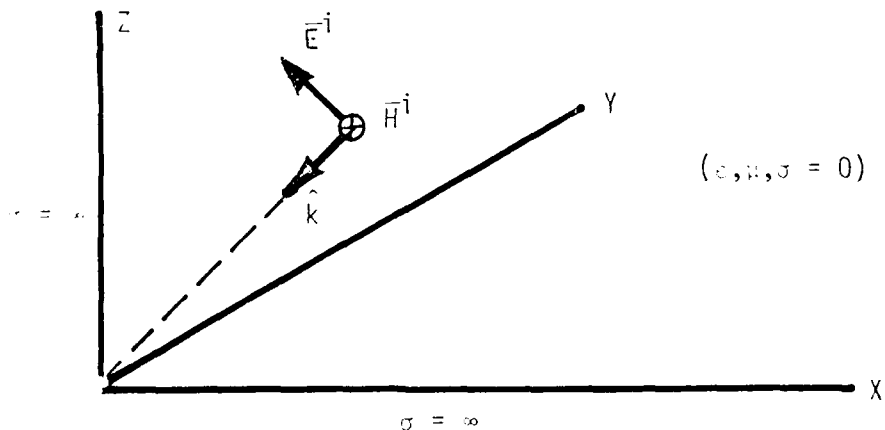


Figure 1.1. Plane wave illumination of a corner reflector.

2. SURFACE CURRENT AND CHARGE DENSITIES FOR POLARIZATION PERPENDICULAR TO THE AXIS OF THE WEDGE

To obtain expressions for surface current density \bar{K} and surface charge density σ let us replace the above problem with an equivalent problem as shown in Figure 2.1. The time dependence $e^{j\omega t}$ will be understood throughout the report. Then:

$$\bar{E}^i(\bar{R}, t) = \text{Re} \left[\bar{E}^i(\bar{R}) e^{j\omega t} \right] = \text{Re} \left[\bar{E}_0^i e^{j(\omega t - \bar{k} \cdot \bar{R})} \right] \quad (2.1)$$

with:

$$\bar{k} = k(-\sin\theta \hat{x} + \cos\theta \hat{z})$$

$$k = \frac{\omega}{c}$$

$$c = \frac{1}{\sqrt{\mu\epsilon}}$$

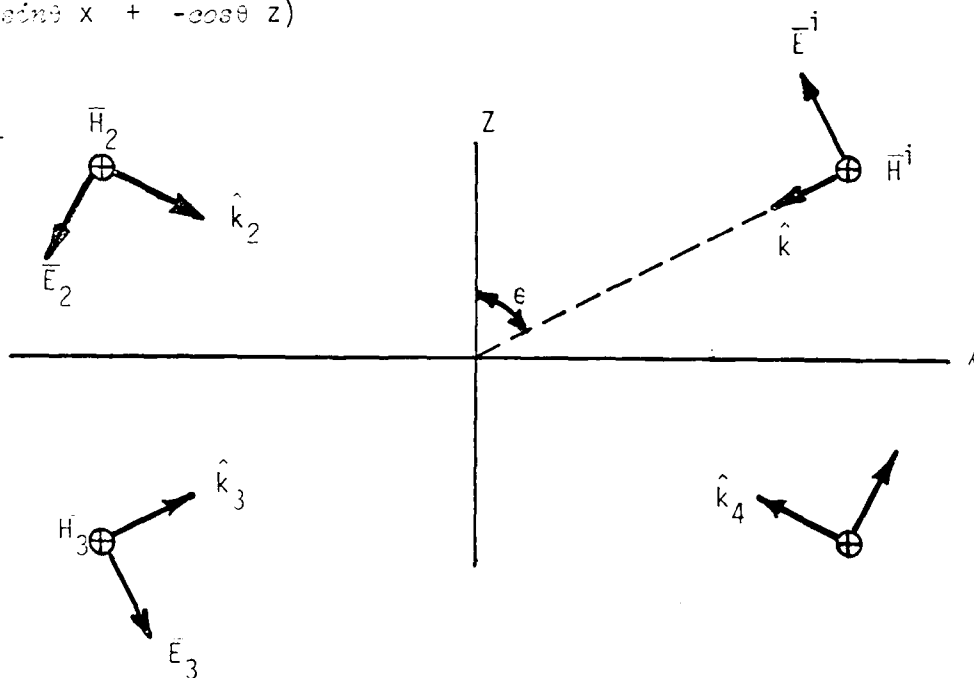


Figure 2.1. Equivalent problem obtained using image fields

$$|\bar{k}_\alpha| = k$$

$$|\bar{E}_{\alpha 0}^i| = E_0^i \quad \alpha = 2, 3, 4$$

$$\left. \begin{aligned}
 \hat{k}_2 &= \sin\theta \hat{x} - \cos\theta \hat{z} \\
 \hat{k}_3 &= \sin\theta \hat{x} + \cos\theta \hat{z} \\
 \hat{k}_4 &= -\sin\theta \hat{x} + \cos\theta \hat{z} \\
 \bar{E}_0^i &= E_0^i (-\cos\theta \hat{x} + \sin\theta \hat{z}) \\
 \bar{E}_{20} &= E_{20} (-\cos\theta \hat{x} - \sin\theta \hat{z}) \\
 \bar{E}_{30} &= E_{30} (\cos\theta \hat{x} - \sin\theta \hat{z}) \\
 \bar{E}_{40} &= E_{40} (\cos\theta \hat{x} + \sin\theta \hat{z})
 \end{aligned} \right\} (2.2)$$

For surface current density we have:

$$\bar{K} = \hat{n} \times \bar{H}_{\text{total}} = \hat{n} \times \frac{1}{\eta} (\hat{k} \times \bar{E}^i + \hat{k}_2 \times \bar{E}_2 + \hat{k}_3 \times \bar{E}_3 + \hat{k}_4 \times \bar{E}_4)$$

where:

$$\eta = \sqrt{\mu/\epsilon}$$

is the intrinsic impedance of air. On the surface $x > 0, z = 0$ we have:

$$\left. \begin{aligned}
 \bar{K}(\bar{R}) &= \hat{z} \times \frac{1}{\eta} (\hat{k} \times \bar{E}_0^i + \hat{k}_4 \times \bar{E}_{40}) e^{jkx\sin\theta} + (\hat{k}_2 \times \bar{E}_{20} + \hat{k}_3 \times \bar{E}_{30}) e^{-jkx\sin\theta} \\
 &= -\hat{x} 2H_0^i (e^{jkx\sin\theta} + e^{-jkx\sin\theta}) \\
 &= -\hat{x} 4H_0^i \cos(kx\sin\theta)
 \end{aligned} \right\} (2.3)$$

on the surface $x = 0, z > 0$ we have:

$$\bar{K}(\bar{R}) = \hat{x} \times \hat{y} H_0^i (2e^{jkz\cos\theta} + 2e^{-jkz\cos\theta}) = \hat{z} 4H_0^i \cos(kz\cos\theta) \quad (2.4)$$

To obtain the surface charge density σ we will make use of a boundary

condition derived from the continuity equation. When one of the media is a perfectly conducting surface this boundary condition reads:

$$\nabla \cdot \bar{K} = -j\omega\sigma$$

Therefore, on the surface $x > 0, z = 0$, we have:

$$\begin{aligned} \sigma(\bar{R}) &= \frac{j}{\omega} 4H_0^i k_2 \sin\theta \sin(kx_2 \sin\theta) \\ \sigma(\bar{R}) &= j4\epsilon E_0^i \sin\theta \sin(kx_2 \sin\theta) \end{aligned} \quad (2.5)$$

similarly on the surface $x = 0, z > 0$ we have:

$$\sigma(\bar{R}) = -j4\epsilon E_0^i \cos\theta \sin(kz_2 \cos\theta) \quad (2.6)$$

2.1. Surface current and charge densities for polarizations parallel to the wedge axis

For this polarization as it is apparent from Figure 2.2 the following changes should be made in the formulation of the previous section:

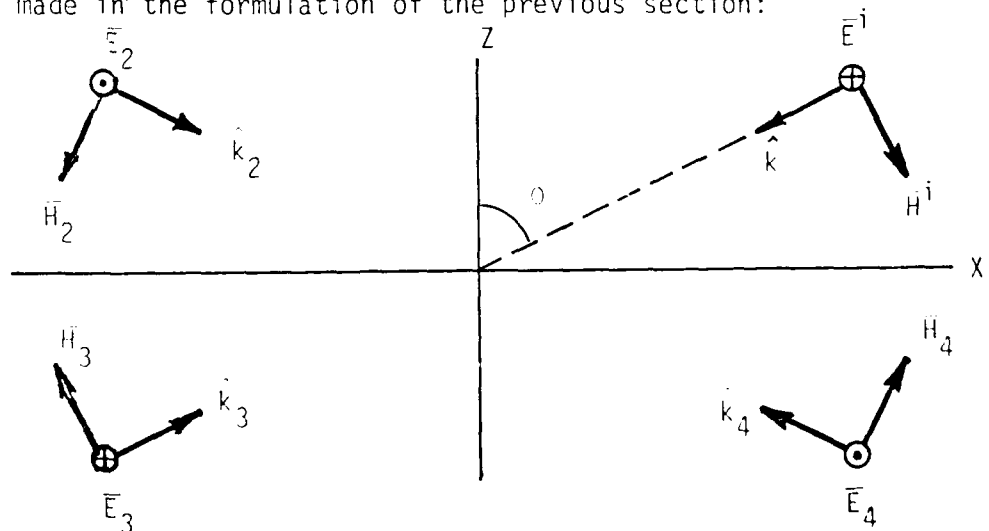


Figure 2.2. Equivalent problem obtained by using image field.

$$\bar{H}_0^i = H_0^i (\cos\theta \hat{x} - \sin\theta \hat{z})$$

$$\bar{H}_{20} = H_0^i (-\cos\theta \hat{x} - \sin\theta \hat{z})$$

$$\bar{H}_{30} = H_0^i (-\cos\theta \hat{x} + \sin\theta \hat{z})$$

$$\bar{H}_{40} = H_0^i (\cos\theta \hat{x} + \sin\theta \hat{z})$$

$$\bar{K}(\bar{R}) = \hat{y} j 4 H_0^i \cos\theta \sin(kx \sin\theta) \quad x > 0, z = 0 \quad (2.7)$$

$$\bar{K}(\bar{R}) = \hat{y} j 4 H_0^i \sin\theta \sin(kz \cos\theta) \quad x = 0, z > 0 \quad (2.8)$$

$$g(\bar{R}) = 0 \quad \text{for either } x > 0, z = 0 \text{ or } x = 0, z > 0 \quad (2.9)$$

3. OPEN CIRCUIT VOLTAGE OF A SHORT MONOPOLE MOUNTED ON THE RIGHT-ANGLE CORNER REFLECTOR

The geometry of the problem and the significant parameters are shown in Figure 3.1. We assume that the probe is electrically small. We will

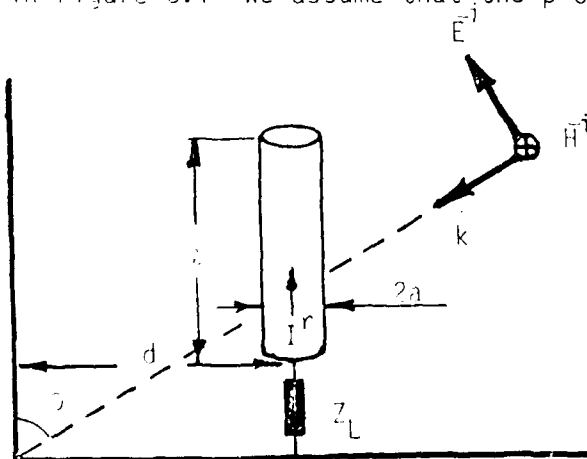


Figure 3.1. Short monopole mounted on a wedge.

consider only the non-trivial polarization of the incident field. As a result of the image theorem, the induced current in the receiving antenna is related to the open circuit voltage by:

$$I^r = \frac{V_{oc}^r}{Z_{in}^t / 2 + Z_L} \quad (3.1)$$

where:

I^r = current at the base of the receiving antenna

Z_{in}^t = input impedance of two transmitting parallel dipole antennas resulted by removing both conducting planes and using the image probes.

V_{oc}^r = open circuit voltage of the receiving monopole

In this section we will deal with open circuit voltage only. The input impedance problem will be discussed in a separate section. Using the vector effective height \vec{h}^t of an antenna, we can write:

$$V_{oc}^r = \vec{E}^i \cdot \vec{h}^t \quad (3.2)$$

The vector effective height of a short dipole (or equivalently a monopole on a ground plane) is given by:

$$\vec{h}^t(\vec{R}) = -z \sin\theta \hat{\theta}$$

which corresponds to a linear current distribution:

$$I^t(z) = I_0(1 - |z|/a) \quad |z| \leq a, \text{ with } ka \ll 1.$$

For the problem at hand we have:

$$V_{oc}^r = \left. \vec{E}^i(\vec{R}') \cdot \vec{h}^t(\vec{R}) \right|_{(R' = d, \theta' = \frac{\pi}{2}, \phi' = 0)} = (-ka \sin \theta \hat{\theta})$$

$$\cdot \vec{E}_0^i e^{jkda \sin \theta} + ka \sin \theta \hat{z} \cdot \vec{E}_{20} e^{-jkda \sin \theta}$$

or

$$V_{oc}^r = j2E_0^i ka \sin \theta \cos(kda \sin \theta) \quad (3.3)$$

3.1. Open circuit voltage of a semi-loop probe whose axis is parallel to the wedge axis

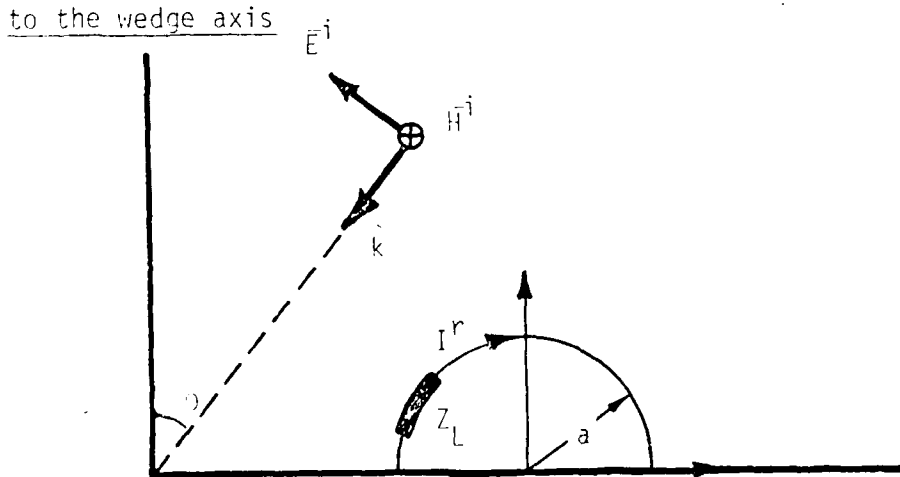


Figure 3.2. Small semi-loop mounted on the wedge.

The open circuit voltage for the probe shown in figure 3.2 is defined as:

$$V_{OC}^r = -\sum \vec{E}^i \cdot \vec{h}^t$$

For a small loop with const current distribution \vec{h}^t is given by:

$$\vec{h}^t(\vec{R}) = j \frac{\pi}{k} (ka)^2 \sin\theta \hat{\theta}$$

$$V_{OC}^r = -\sum \vec{E}^i(\vec{R}') \cdot \vec{h}^t(\vec{R}) \Big|_{(R' = d, \theta' = \frac{\pi}{2}, \phi' = 0)}$$

$$V_{OC}^r = -\frac{1}{k} \left\{ j\pi(ka)^2 \sin\frac{\pi}{2} (-\hat{\theta}) \cdot \vec{E}_0^i e^{jkda\sin\theta} \right. \\ \left. + j\pi(ka)^2 \sin\frac{\pi}{2} (-\hat{\theta}_2) \cdot \vec{E}_{20}^i e^{-jkda\sin\theta} \right\}$$

$$V_{OC}^r = -j2\pi(ka)^2 \frac{E_0^i}{k} \cos(kda\sin\theta)$$

$$= -j2\pi(ka)^2 H_{0\cos}^i(kda\sin\theta) \quad (3.4)$$

3.2. Open circuit voltage of a semi loop probe whose axis is perpendicular to the wedge axis.

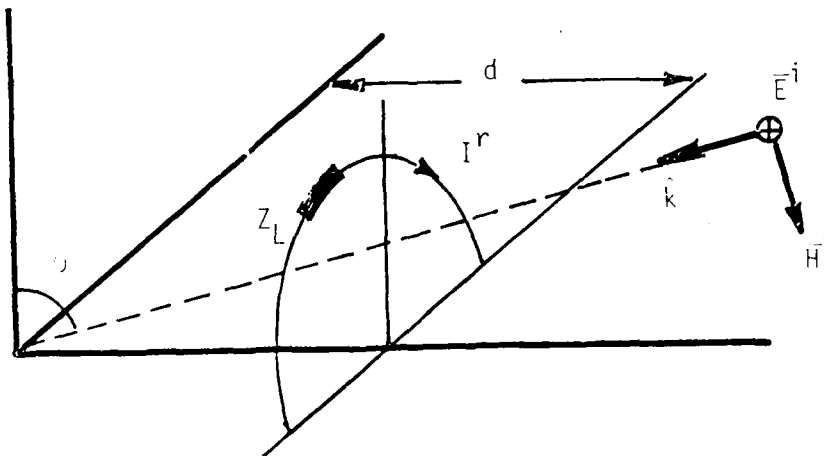


Figure 3.3 Small semi-loop probe with axis perpendicular to the wedge axis.

The pertinent polarization of the incident field for this configuration of probe is depicted in Figure 3.3. Following the same procedures of the previous section and considering the direction of the current density of probe we can write:

$$V_{OC}^r = - \sum \vec{E}^i \cdot \vec{h}^t \Big|_{(R' = d, \theta' = \frac{\pi}{2}, \phi' = 0)}$$

$$V_{OC}^r = - 2\omega(\mu\pi a^2) H_0^i \cos\theta \sin(kd \sin\theta) \quad (3.5)$$

4. INPUT IMPEDANCE OF THE PROBES

Equation (3.1) of section 3. indicates that for completion of the equivalent circuit parameters we need to evaluate Z_{in}^t , which will be simply referred as Z_{in} from now on, in each of the probing configurations considered previously. Let us once more recall that Z_{in} is the input impedance of the transmitting antenna in the presence of its images. With this in mind we will begin deriving analytical formulas for the input impedance functions involved in the problems at hand under the assumptions imposed on electrical sizes of the probes. The problem of determining the impedance for the cases considered here has been extensively explored previously, however most often in the form of tables and curves. We will include here the complete expressions for these functions.

4.1. Impedance parameters of two identical, parallel, and short transmitting dipoles.

The problem arising from the application of image theory to two antisymmetrically driven antenna is shown in figure 4.1. Since the probe is assumed to be thin and short ($a \ll \lambda$, $k\lambda \ll 1$), a linear current distribution is a suitable

approximation and the induced EMF method can be applied successfully to determine its input impedance.

For convenience we will proceed by assuming a sinusoidal current distribution. At the final stages the results will be simplified by using the conditions imposed on a , λ , and ρ .

Based on filamentary current distribution we have for the magnetic vector potential $\vec{A}(\vec{R})$:

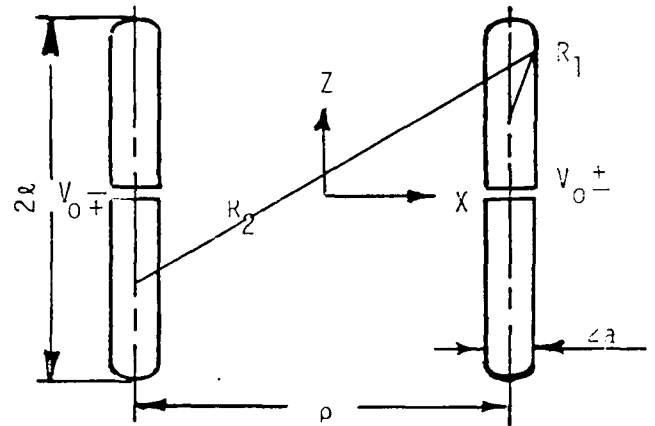


Figure 4.1

Two identical, parallel transmitting antennas.

$$\begin{aligned} \vec{A}(\vec{R}) &= \frac{\mu}{4\pi} \int_{V'} G(\vec{R}|\vec{R}') \vec{J}(\vec{R}') dv' = \\ &= \hat{z} \frac{\mu}{4\pi} \int_{-a}^a I(z') \left\{ \frac{e^{-jkR_1}}{R_1} - \frac{e^{-jkR_2}}{R_2} \right\} dz' \end{aligned}$$

R_1 and R_2 are the instances from the observation point to the source points on the axes of the dipoles. For \vec{R} on the surface of one of the antennas we have:

$$R_1 = \sqrt{[(z - z')^2 + a^2]} \quad R_2 = \sqrt{[(z - z')^2 + \rho^2]} \quad \text{for } \rho \gg a. \quad (4.1)$$

The electric field on the surface of right hand side antenna is given by:

$$\begin{aligned} \vec{E} &= -j\omega \left(1 + \frac{1}{k^2} \nabla \cdot \nabla \right) \vec{A} = -\hat{z} j\omega \left(1 + \frac{1}{k^2} \frac{\partial^2}{\partial z^2} \right) A_z(z) \\ &= -\hat{z} V_0 \delta(z) \end{aligned} \quad (4.2)$$

where as usual a slice generator has been assumed. Multiplying (4.2) by $I(z)$

and integrating over the source region we obtain

$$V_0 I(0) = \frac{j\omega\mu}{4\pi} \int_{-l}^l \int_{-l}^l I(z) I(z') \left(1 + \frac{1}{k^2} \frac{\partial^2}{\partial z^2}\right) (G_1 - G_2) dz dz'$$

$$\text{where } G_1(z, z') = \frac{e^{-jkR_1}}{R_1} \quad G_2(z, z') = \frac{e^{-jkR_2}}{R_2}$$

$$G(z, z') = G_1(z, z') - G_2(z, z')$$

The first integration with respect to z amounts for evaluation of z -component of the near zone electric field due to current distribution of the form:

$$I(z) = I_m \sin k(\ell - |z|) \quad |z| \leq \ell$$

Therefore it is given by [5.1]:

$$\int_{-l}^l I(z) \left(1 + \frac{1}{k^2} \frac{\partial^2}{\partial z^2}\right) G(z, z') dz = \frac{I_m}{k} \{G(\ell, z') + G(-\ell, z') - 2 \cos k\ell G(0, z')\}$$

we then have:

$$Z_{in} I^2(0) = \frac{j\omega\mu I_m}{4\pi k} \int_{-l}^l \{G(\ell, z') + G(-\ell, z') - 2 \cos k\ell G(0, z')\} I(z') dz'$$

$$Z_{in} = \frac{j\eta}{2\pi \sin^2 k\ell} \int_0^\ell \{G(\ell, z) + G(-\ell, z) - 2 \cos k\ell G(0, z)\} \times \sin k(\ell - z) dz \quad (4.3)$$

Let us note that from the circuit relations for these antennas:

$$V_1 = Z_{11}I_1 + Z_{12}I_2$$

$$V_2 = Z_{21}I_1 + Z_{22}I_2$$

It follows that for antisymmetrically driven antennas we have:

$$Z_{in} = Z_{11} - Z_{12} \quad (4.4)$$

Let us define:

$$\zeta(a) = \int_0^l \{G_1(l, z) + G_1(-l, z) - 2\cos kl G_1(0, z)\} \times \\ \times \sin k(l - z) dz \quad (4.5)$$

combining (4.3) - (4.5) we obtain:

$$Z_{11} = \frac{j\eta}{2\pi \sin^2 kl} \zeta(a) \quad Z_{12} = \frac{j\eta}{2\pi \sin^2 kl} \zeta(\rho) \quad (4.6)$$

Therefore the problem of input impedance reduces to the evaluation of $\zeta(a)$, and $\zeta(\rho)$.

$\zeta(a)$ has been previously evaluated by expressing it in terms of sine and cosine-integrals [6]. We will choose another approach which enables us to obtain a series expansion for $\zeta(a)$, and $\zeta(\rho)$ and in particular to reduce the results to simplified forms under certain assumptions on the parameters. We have:

$$\int_0^{\ell} G_1(\ell, z) \sin k(\ell - z) dz = \int_0^{\ell} \frac{e^{-jk\sqrt{x^2 + a^2}}}{\sqrt{x^2 + a^2}} \sin kx dx$$

$$\int_0^{\ell} G_1(-\ell, z) \sin k(\ell - z) dz = \int_{\ell}^{2\ell} \frac{e^{-jk\sqrt{x^2 + a^2}}}{\sqrt{x^2 + a^2}} \sin k(2\ell - x) dx$$

$$\int_0^{\ell} G_1(0, z) \sin k(\ell - z) dz = \int_0^{\ell} \frac{e^{-jk\sqrt{x^2 + a^2}}}{\sqrt{x^2 + a^2}} \sin k(\ell - x) dx$$

Therefore we are led to define:

$$s(\xi, a) = \int_0^{\ell} \frac{e^{-k\sqrt{x^2 + a^2}}}{\sqrt{x^2 + a^2}} \sin kx dx \quad (4.7)$$

$$c(\xi, a) = \int_0^{\ell} \frac{e^{-jk\sqrt{x^2 + a^2}}}{\sqrt{x^2 + a^2}} \cos kx dx \quad (4.8)$$

Then in terms of $s(\ell, a)$ and $C(\ell, a)$ we can write:

$$\begin{aligned} \zeta(a) &= s(\ell, a) + \sin 2k\ell (C(2\ell, a) - C(\ell, a)) + \\ &\quad - \cos 2k\ell (s(2\ell, a) - s(\ell, a)) - 2\sin k\ell \cos k\ell C(\ell, a) + 2 \cos^2 k\ell s(\ell, a) \\ \xi(a) &= 2 s(\ell, a) + (2 s(\ell, a) - s(2\ell, a)) \cos 2k\ell - (2C(\ell, a) - C(2\ell, a)) \sin 2k\ell \end{aligned} \quad (4.9)$$

In order to evaluate $s(\ell, a)$ and $c(\ell, a)$ let us introduce the following dimensionless parameters:

$$\xi = k\ell, \quad \alpha = \frac{a}{\ell}, \quad \beta = \sqrt{1 + \alpha^2} \quad (4.10)$$

Then:

$$s(\ell, a) = \int_0^1 \frac{e^{-j\xi\sqrt{x^2 + \alpha^2}}}{\sqrt{x^2 + \alpha^2}} \sin \xi x dx \equiv s(\xi, \alpha) \quad (4.7')$$

$$c(\ell, a) = \int_0^1 \frac{e^{-j\xi\sqrt{x^2 + \alpha^2}}}{\sqrt{x^2 + \alpha^2}} \cos \xi x dx \equiv c(\xi, \alpha) \quad (4.8')$$

with:

$$\frac{\partial S}{\partial \xi} = -j \int_0^1 e^{-j\xi\sqrt{x^2 + \alpha^2}} \sin \xi x dx + \int_0^1 \frac{x e^{-j\xi\sqrt{x^2 + \alpha^2}}}{\sqrt{x^2 + \alpha^2}} \cos \xi x dx$$

$$\int_0^1 \frac{x e^{-j\xi\sqrt{x^2 + \alpha^2}}}{(x^2 + \alpha^2)} \cos \xi x dx = -\frac{1}{j} e^{-j\xi\sqrt{x^2 + \alpha^2}} \cos \xi x \Big|_0^1 -$$

$$-\frac{1}{j} \int_0^1 e^{-j\xi\sqrt{x^2 + \alpha^2}} \sin \xi x dx$$

Hence:

$$\frac{\partial S}{\partial \xi} = -\frac{1}{j\xi} e^{-j\xi\sqrt{x^2 + \alpha^2}} \cos \xi x \Big|_0^1 = -\frac{1}{j\xi} (e^{-j\xi\beta} \cos \xi - e^{-j\alpha\xi})$$

similarly:

$$\frac{\partial C}{\partial \xi} = -j \int_0^1 e^{-j\xi\sqrt{x^2 + \alpha^2}} \cos \xi x dx - \int_0^1 \frac{x e^{-j\xi\sqrt{x^2 + \alpha^2}}}{\sqrt{x^2 + \alpha^2}} \times \sin \xi x dx$$

$$\frac{\partial C}{\partial \xi} = \frac{1}{j\xi} e^{-j\xi\sqrt{x^2 + \alpha^2}} \sin \xi x \Big|_0^1 = \frac{1}{j\xi} e^{-j\xi\beta} \sin \xi \quad (4.12)$$

We will proceed by finding a series expansion for $\frac{\partial S}{\partial \xi}$ and $\frac{\partial C}{\partial \xi}$. For the sake of numerical computation we will develop two different series expansion depending on the relative values of $\alpha\xi = ka$.

I) $\alpha\xi \ll 1$

$$\frac{\partial S}{\partial \xi} = -\frac{1}{j\xi} \left\{ \frac{1}{2} (e^{-j\xi(\beta-1)} + e^{-j\xi(\beta+1)}) - e^{-j\xi\alpha} \right\}$$

$$= \frac{1}{2} \sum_{n=1}^{\infty} \frac{(-j\xi)^{n-1}}{n!} \{ (\beta-1)^n + (\beta+1)^n - 2\alpha^n \}$$

$$s(\xi, \alpha) = -\frac{1}{j2} \sum_{n=1}^{\infty} \frac{(-j\xi)^n}{n!n} \{ (\beta-1)^n + (\beta+1)^n - 2\alpha^n \} \quad (4.13)$$

$$2s(\xi, \alpha) - s(2\xi, \frac{\alpha}{2}) = -\frac{1}{j2} \sum_{n=1}^{\infty} \frac{(-j2\xi)^n}{n!n} s_n$$

$$s_n = 2^{1-n} \{(\beta-1)^n + (\beta+1)^n\} - \{(\beta(\frac{\alpha}{2})-1)^n + (\beta(\frac{\alpha}{2})+1)^n\} - 2^{1-n} \alpha^n .$$

(4.14)

Similarly we have:

$$\frac{\partial c}{\partial \xi} = \frac{1}{j\xi} e^{-j\xi\beta} \sin n\xi = \frac{j}{2} \sum_{n=1}^{\infty} \frac{(-j\xi)^{n-1}}{n!} \{(\beta-1)^n - (\beta+1)^n\}$$

$$c(\xi, \alpha) - c(0, \alpha) = -\frac{1}{2} \sum_{n=1}^{\infty} \frac{(-j\xi)^n}{n!n} \{(\beta-1)^n - (\beta+1)^n\}$$

$$c(0, \alpha) = \int_0^1 \frac{d\alpha}{\sqrt{x^2 + \alpha^2}} = c_n(x + \sqrt{x^2 + \alpha^2}) \Big|_0^1 = \ln \frac{\beta+1}{\alpha}$$

$$c(\xi, \alpha) = \ln \frac{\beta+1}{\alpha} - \frac{1}{2} \sum_{n=1}^{\infty} \frac{(-j\xi)^n}{n!n} \{(\beta-1)^n - (\beta+1)^n\} \quad (4.15)$$

$$2c(\xi, \alpha) - c(2\xi, \frac{\alpha}{2}) = \ln \frac{2[\beta(\frac{\alpha}{2})+1]}{(\beta+1)^2} + \ln \alpha - \frac{1}{2} \sum_{n=1}^{\infty} \frac{(-j2\xi)^n}{n!n} c_n$$

(4.16)

$$c_n = 2^{1-n} [(\beta-1)^n - (\beta+1)^n] - [(\beta(\frac{\alpha}{2})-1)^n - (\beta(\frac{\alpha}{2})+1)^n] .$$

The previous expressions are so far exact. Let us introduce approximations under the assumptions:

$$\alpha = \frac{a}{2} \ll 1 \quad \xi = k\ell \ll 1$$

then

$$\beta(\alpha) = 1 + \frac{1}{2} \alpha^2 + 0(\alpha^4)$$

$$\ln \frac{2[\beta(\frac{\alpha}{2})+1]}{(\beta(\alpha)+1)^2} = \ln 4(1 + \frac{\alpha^2}{16} + \dots) - 2 \ln 2(1 + \frac{\alpha^2}{4} + \dots) = 0(\alpha^2)$$

$$s_n = 2^{1-n} \sum_{m=0}^n \binom{n}{m} \beta^m [1 + (-1)^{n-m}] - \sum_{m=0}^n \binom{n}{m} \beta^m (\frac{\alpha}{2})^m \times$$

$$x [1 + (-1)^{n-m}] - 2^{1-n} \alpha^n$$

$$2^{1-n} \beta^m(\alpha) - \beta^m\left(\frac{\alpha}{2}\right) = 2^{1-n}(1 + \alpha^2)^{\frac{m}{2}} - \left(1 + \frac{\alpha^2}{4}\right)^{\frac{m}{2}} =$$

$$= (2^{1-n} - 1) + o(\alpha^2)$$

$$a_n = \sum_{m=0}^n (2^{1-n} - 1) \binom{n}{m} [1 + (-1)^{n-m}] - \alpha \delta_{n1} + o(\alpha^2)$$

$$= (2^{1-n} - 1) 2^n + o(\alpha^2) = (2 - 2^n) - \alpha \delta_{n1} + o(\alpha^2)$$

where δ_{n1} is the Kronecker delta.

$$c_n = -2^{1-n} \sum_{m=0}^n \binom{n}{m} \beta^m [1 - (-1)^{n-m}] + \sum_{m=0}^n \binom{n}{m} \beta^m\left(\frac{\alpha}{2}\right) [1 - (-1)^{n-m}]$$

$$= (2^n - 2) + o(\alpha^2)$$

Thus we have the following approximations:

$$s(\xi, \alpha) = \frac{1}{j2} \left\{ \sum_{n=1}^{\infty} \frac{(-j2\xi)^n}{n!n} + j2\alpha\xi \right\} + o(\alpha^2\xi) \quad (4.13')$$

$$2s(\xi, \alpha) - s(2\xi, \frac{\alpha}{2}) = \frac{1}{2j} \left\{ \sum_{n=1}^{\infty} \frac{(-j2\xi)^n}{n!n} (2^n - 2) - j2\alpha\xi \right\} \quad (4.14')$$

$$+ o(\alpha^2\xi) \quad (4.14')$$

$$2c(\xi, \alpha) - c(2\xi, \frac{\alpha}{2}) = 2n\alpha - \frac{1}{2} \sum_{n=1}^{\infty} \frac{(-j2\xi)^n}{n!n} (2^n - 2) + o(\alpha^2\xi) \quad (4.16')$$

Finally for $\zeta(a)$ we obtain:

$$\zeta(a) = \sin 2\xi 2n\alpha + (\sin 2\xi - j\cos 2\xi) \sum_{n=1}^{\infty} \frac{(-j2\xi)^n}{n!n} \times$$

$$\times (2^{n-1} - 1) + j \sum_{n=1}^{\infty} \frac{(-j2\xi)^n}{n!n} - (2 + \cos 2\xi)\alpha\xi + o(\alpha^2\xi)$$

$$\zeta(a) = 2\xi - \frac{5}{36}(2\xi)^3 - 3\alpha\xi + \sin 2\xi 2n\alpha - \frac{j}{48}(2\xi)^4 +$$

$$+ o(\max\{\xi^5, \alpha^2\xi\}) \quad (4.17)$$

II) $\alpha\xi \gg 1$

For this case we have $\xi = k\lambda$, $\alpha = \frac{\beta}{\lambda}$. Following the above formulations we set:

$$s(\xi, \alpha) = s(0, \alpha) + e^{-j\xi\alpha} \sum_{n=0}^{\infty} s_n \xi^n \quad (4.18)$$

$$c(\xi, \alpha) = c(0, \alpha) + e^{-j\xi\alpha} \sum_{n=0}^{\infty} c_n \xi^n. \quad (4.19)$$

Then:

$$\begin{aligned} \frac{\partial s}{\partial \xi} &= e^{-j\xi\alpha} \sum_{n=1}^{\infty} n s_n \xi^{n-1} - j\alpha e^{-j\xi\alpha} \sum_{n=0}^{\infty} s_n \xi^n = \\ &= e^{-j\xi\alpha} \sum_{n=0}^{\infty} [-j\alpha s_n + (n+1)s_{n+1}] \xi^n = \\ &= -\frac{1}{j\xi} (e^{-j\xi\beta} \cos \alpha \xi - e^{-j\xi\alpha}) = \frac{e^{-j\xi\alpha}}{j2\xi} \sum_{n=1}^{\infty} \frac{(-j\xi)^n}{n!} \times \\ &\quad \times \{(\beta - \alpha - 1)^n + (\beta - \alpha + 1)^n\} \\ &= e^{-j\xi\alpha} \sum_{n=1}^{\infty} \frac{(-j\xi)^{n-1}}{n!} \sigma_n = e^{-j\xi\alpha} \sum_{n=0}^{\infty} \frac{(-j\xi)^n}{(n+1)!} \sigma_{n+1} \end{aligned}$$

where we have defined:

$$\sigma_n = \frac{1}{2} \{(\beta - \alpha - 1)^n + (\beta - \alpha + 1)^n\}; \quad n=0, 1, 2, \dots \quad (4.20)$$

Therefore we have:

$$-j\alpha s_n + (n+1)s_{n+1} = (-j)^n \frac{\sigma_{n+1}}{(n+1)!}; \quad n=0, 1, 2, 3, \dots \quad (4.21)$$

Recursion relation (4.21) starts off from $s_0 = 0$ which is an immediate consequence of (4.18):

$$s_0 = 0$$

$$s_1 = \sigma_1$$

$$s_2 = -\frac{j}{2!} \left(\frac{\sigma_2}{2} - \frac{\alpha \sigma_1}{1} \right)$$

$$\alpha = \frac{\epsilon}{2} \ll 1, \quad \xi \ll 1.$$

We have:

$$\beta - \alpha = \sqrt{1+\alpha^2} - \alpha = \sum_{m=1}^{\infty} (-1)^{m+1} \frac{(2m-3)!!}{2^m m!} \alpha^{-(2m-1)}$$

with:

$$(2m-3)!! = (2m-3)(2m-5) \dots 3 \cdot 1 \quad m=2,3,\dots$$

$$(-1)!! = 1$$

$$\sigma_n = \frac{1}{2} \{ (\beta - \alpha + 1)^n + (\beta - \alpha - 1)^n \} = \frac{1}{2} \sum_{m=0}^n \binom{n}{m} (\beta - \alpha)^m [1 + (-1)^{n-m}]$$

$$\gamma_n = \frac{1}{2j} \{ (\beta - \alpha + 1)^n - (\beta - \alpha - 1)^n \} = \frac{1}{2j} \sum_{m=0}^n \binom{n}{m} (\beta - \alpha)^m [1 - (-1)^{n-m}]$$

$$\begin{aligned} (\beta - \alpha)^m &= \left(\frac{1}{2} \alpha^{-1}\right)^m \left(1 + \sum_{r=0}^{\infty} (-1)^{r+1} \frac{(2r+1)!!}{2^{r+1} (r+2)!} \alpha^{-(2r+2)}\right)^m \\ &= \left(\frac{1}{2} \alpha^{-1}\right)^m \left(1 + m \sum_{r=0}^{\infty} (-1)^{r+1} \frac{(2r+1)!!}{2^{r+1} (r+2)!} \alpha^{-(2r+2)} + \right. \\ &\quad \left. + \frac{m(m-1)}{2} \frac{\alpha^{-4}}{16} \left(1 + \sum_{r=0}^{\infty} (-1)^{r+1} \frac{(2r+3)!!}{2^r (r+3)!} \alpha^{-(2r+2)}\right)^2 + \dots\right) \end{aligned}$$

$$\beta - \alpha = \frac{1}{2} \alpha^{-1} \left(1 - \frac{1}{4} \alpha^{-2} + \frac{1}{8} \alpha^{-4} - \frac{5}{64} \alpha^{-6}\right) + 0(\alpha^{-9})$$

$$(\beta - \alpha)^2 = \frac{1}{2} \alpha^{-2} \left(1 - \frac{1}{2} \alpha^{-2} + \frac{5}{16} \alpha^{-4}\right) + 0(\alpha^{-8})$$

$$(\beta - \alpha)^3 = \frac{1}{8} \alpha^{-3} \left(1 - \frac{3}{4} \alpha^{-2}\right) + 0(\alpha^{-7})$$

$$(\beta - \alpha)^4 = \frac{1}{16} \alpha^{-4} + 0(\alpha^{-6})$$

$$\sigma_1 = (\beta - \alpha) = \frac{1}{2} \alpha^{-1} - \frac{1}{8} \alpha^{-3} + \frac{1}{16} \alpha^{-5} - \frac{5}{128} \alpha^{-7} + 0(\alpha^{-9})$$

$$\sigma_2 = 1 + (\beta - \alpha)^2 = 1 + \frac{1}{4} \alpha^{-2} - \frac{1}{8} \alpha^{-4} + \frac{5}{64} \alpha^{-6} + 0(\alpha^{-8})$$

$$\sigma_3 = 3(\beta - \alpha) + (\beta - \alpha)^3 = \frac{3}{2} \alpha^{-1} - \frac{1}{4} \alpha^{-3} + \frac{3}{32} \alpha^{-5} + 0(\alpha^{-7})$$

$$\sigma_4 = 1 + 6(\beta - \alpha)^2 + (\beta - \alpha)^4 = 1 + \frac{3}{2} \alpha^{-2} - \frac{11}{16} \alpha^{-4} + 0(\alpha^{-6}) \quad (4.26)$$

.....

$$r_1 = \frac{1}{j}$$

$$r_2 = \frac{2}{j}(z-x) = \frac{1}{j}(x^{-1} - \frac{1}{4}x^{-3} + \frac{1}{8}x^{-5} - \frac{5}{64}x^{-7}) + o(x^{-9})$$

$$r_3 = \frac{1}{j}[1 + 3(z-x)^2] = \frac{1}{j}(1 + \frac{3}{4}x^{-2} - \frac{3}{8}x^{-4}) + o(x^{-6})$$

$$r_4 = \frac{1}{j}[4(z-x) + 4(z-x)^3] = \frac{1}{j}(2x^{-1}) + o(x^{-5})$$

.....

From (4.22), (4.25) and (4.26) it follows that:

$$c_1(x) = (2x)^{-1} - (2x)^{-3} + o(x^{-5})$$

$$c_2(x) = -\frac{j}{2!} [(2x)^{-2} - 2(2x)^{-4}] + o(x^{-5})$$

$$c_3(x) = -\frac{j}{3!} [\frac{1}{2}(2x)^{-1} + \frac{1}{3}(2x)^{-3}] + o(x^{-5})$$

$$c_4(x) = \frac{j}{4!} [\frac{4}{3}(2x)^{-2} - 2(2x)^{-4}] + o(x^{-5}) \tag{4.27}$$

.....

$$c_1(x) = -j$$

$$c_2(x) = -\frac{1}{2!}(-x + (2x)^{-1} - (2x)^{-3}) + o(x^{-5})$$

$$c_3(x) = \frac{j}{3!}(x^2 - \frac{1}{6} + \frac{3}{2}(2x)^{-2} - 3(2x)^{-4} + o(x^{-5}))$$

$$c_4(x) = \frac{1}{4!}(-x^3 + \frac{x}{6} + \frac{1}{4}(2x)^{-1} + \frac{3}{2}(2x)^{-3} + o(x^{-5}))$$

.....

Also, let us note that:

$$c(0, x) = \ln(x^{-1} + \sqrt{1+x^{-2}}) = \ln(1+x^{-1}) + \sum_{m=1}^{\infty} (-1)^{m+1} x$$

$$x \frac{(2m-3)!!}{2^m m!} x^{-2m}$$

$$c(0, x) = x^{-1} + \sum_{m=1}^n (-1)^{m+1} \frac{(2n-3)!!}{2^m m!} x^{-2n} -$$

$$\begin{aligned}
 & - \frac{1}{2} \left\{ \alpha^{-1} + \sum_{m=1}^{\infty} (-1)^{m+2} \frac{(2m-3)!!}{2^m m!} \alpha^{-2m} \right\}^2 + \dots \\
 & = \alpha^{-1} - \frac{1}{6} \alpha^{-3} + o(\alpha^{-5})
 \end{aligned}$$

$$2c(0, \alpha) - c(0, \frac{\alpha}{2}) = \alpha^{-3} + o(\alpha^{-5}) \tag{4.28}$$

Now we can proceed to evaluate $\zeta(\cdot)$:

$$\begin{aligned}
 \zeta(\cdot) &= 2s(\xi, \alpha) + \cos 2\xi (2s(\xi, \alpha) - s(2\xi, \frac{\alpha}{2})) \\
 &\quad - \sin 2\xi (2c(\xi, \alpha) - c(2\xi, \frac{\alpha}{2})) = \\
 &= e^{-j\xi\alpha} \left\{ \sum_{n=0}^{\infty} (2\xi)^n \{ 2^{1-n} s_n(\alpha) + \cos 2\xi \times \right. \\
 &\quad \times (2^{1-n} c_n(\alpha) - s_n(\frac{\alpha}{2})) - \sin 2\xi (2^{1-n} c_n(\alpha) - \\
 &\quad \left. - c_n(\frac{\alpha}{2})) \} \right\} - \sin 2\xi (2c(0, \alpha) - c(0, \frac{\alpha}{2})) \\
 &= e^{-j\xi\alpha} \left\{ \sum_{n=0}^{\infty} (2\xi)^n \{ 2^{2-n} s_n(\alpha) - s_n(\frac{\alpha}{2}) + \right. \\
 &\quad \left. \left(-\frac{(2\xi)^2}{2} + \frac{(2\xi)^4}{24} - \dots \right) (2^{1-n} s_n(\alpha) - s_n(\frac{\alpha}{2})) \right. \\
 &\quad \left. - (2\xi - \frac{(2\xi)^3}{6} + \dots) (2^{1-n} c_n(\alpha) - c_n(\frac{\alpha}{2})) \} \right\} \\
 &\quad - \sin 2\xi (2c(0, \alpha) - c(0, \frac{\alpha}{2}))
 \end{aligned}$$

$$\begin{aligned}
 \zeta(\cdot) &= e^{-j\xi\alpha} \left\{ \frac{3}{4} \alpha^{-3} (2\xi) + j\frac{3}{8} \alpha^{-2} (2\xi)^2 + (2\xi)^3 \left(\frac{1}{16} \alpha^{-1} \right) + \right. \\
 &\quad \left. + o(\max(\xi \alpha^{-5}, \xi^3 \alpha^{-3})) \right\} \tag{4.29} \\
 &= \alpha^{-3} (2\xi) + o(\max(\alpha^{-3} \xi^3, \alpha^{-5} \xi))
 \end{aligned}$$

noting that:

$$\alpha = \frac{2k}{2\xi}$$

we can write:

$$z(\cdot) = \frac{1}{32} e^{-jk_0 a} (2\xi)^4 \{ (k_0 a)^{-1} + j3(k_0 a)^{-2} + 3(k_0 a)^{-3} \} \\ - \frac{1}{8} (2\xi)^4 (k_0 a)^{-3} + 0\{\max(\xi a^{-5}, \xi^3 a^{-3})\} \quad (4.30)$$

using (4.6) together with (4.17) and (4.30) we finally obtain expressions for z_{11} and z_{12} :

$$z_{11} = \frac{j\eta}{2\pi a \sin^2 \xi} z(a) = \frac{j\eta}{2\pi} \xi^{-2} (1 - \frac{\xi^2}{6} + \frac{\xi^4}{24} + \dots)^{-2} \times z(a) \\ = \frac{j\eta}{2\pi} (\xi^{-2} + \frac{1}{3} + 0(\xi^4)) z(a) \\ z_{11} = \frac{j\eta}{2\pi} \{ (4 - 6\alpha)(2\xi)^{-1} - (\frac{2}{9} + \frac{\alpha}{2})(2\xi) + \\ 2\alpha t \xi \ln \alpha - \frac{j}{12} (2\xi)^2 \} + 0\{\max(\xi^3, \alpha^2 \xi^{-1})\}$$

with

$$\alpha = \frac{a}{\lambda}, \quad \xi = k_0 a \quad (4.31)$$

$$z_{12} = \frac{j\eta}{2\pi a \sin^2 \xi} z(\cdot) = \frac{j\eta}{2\pi} (\xi^{-2} + \frac{1}{3} + 0(\xi^4)) z(\cdot) \\ z_{12} = \frac{1}{8} e^{-jk_0 a} (2\xi)^2 \{ (k_0 a)^{-1} + j3(k_0 a)^{-2} + 3(k_0 a)^{-3} \} \\ - \frac{1}{2} (2\xi)^2 (k_0 a)^{-3} + 0\{\xi^4 \max\{(k_0 a)^{-3}, (k_0 a)^{-5}\}\}.$$

Then the input impedance for the problem at hand is given by:

$$z_{in} = z_{11} - z_{12} \quad (4.4)$$

Let us note that in (4.32), as in previous sections, we have $\alpha = 2d$.

4.2 Input impedance of two coaxial small circular loops in transmitting mode.

For an electrically small loop we assume that its current distribution is uniform when driven by a localized voltage. The conventional

induced EMF method will be applied to determine its impedance. However, the formation is much more complicated than the case for linear antennas. Therefore assumptions imposed on the geometry of the probing antennas justify adoption of simpler approximate methods in ad hoc bases for evaluation of self and mutual impedances.

As can be seen from the application of the EMF method to the antennas of previous the previous section the self impedance can be obtained

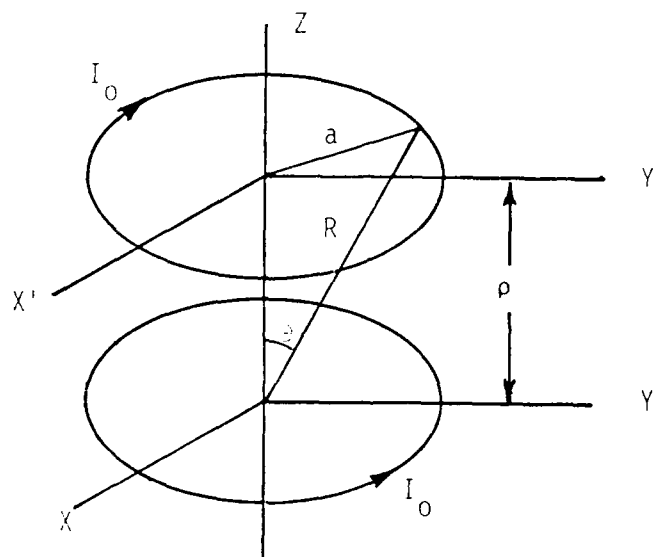


Figure 4.2 Coaxial transmitting loop antennas

by removing the image of one antenna and evaluating the input impedance of the isolated loop.

The input resistance of a constant current loop may be simply evaluated by an application of Poynting's theorem [9.2]. The result is:

$$R_{in} = \frac{\eta}{6\pi} (\pi(ka)^2)^2. \quad (4.33)$$

A rather simple way of obtaining a compact formula for the input reactance of the loop is to make use of the reactance of the loop based on the circuit theory. According to Reference [9.1] the reactance of the loop is given by:

$$x_{in} = \omega(L_i + L_0) \approx \omega \left\{ \frac{1}{8\pi} + a \left(2n \frac{8a}{b} - 2 \right) \right\} \quad (4.34)$$

where L_i is the internal inductance of the wire, L_0 is the so called selected mutual inductance, and b is the radius of the wire of the loop antenna. This result compares very well with the leading term of the formula obtained for x_{in} by application of the wave theory as discussed in [1]. Combining (4.33) and (4.34) we obtain the self impedance of the loop:

$$z_{11} \approx R_{in} + j x_{in} \approx \frac{\pi}{6\pi} (\pi(ka)^2)^2 + j\omega \left\{ \frac{1}{8\pi} + a \left[2n \left(\frac{8a}{b} \right) - 2 \right] \right\} \quad (4.35)$$

4.3 Mutual impedance of the two coaxial loop antennas

As for the case of monopole on a corner reflector, we will present a simple and compact formulation for z_{12} of two small coaxial loop antennas. We will use the EMF method again and therefore the Fresnel field of a constant current loop is needed.

The Fresnel field of a constant current loop antenna has been previously obtained in the form of a rapidly converging power series in [10.1], [8], [3], and [4]. We will obtain another series expansion which closely follows the ones given in [8] and will prove more suitable-

ble in application of the EMF method.

Using the addition theorem for Legendre and spherical Bessel

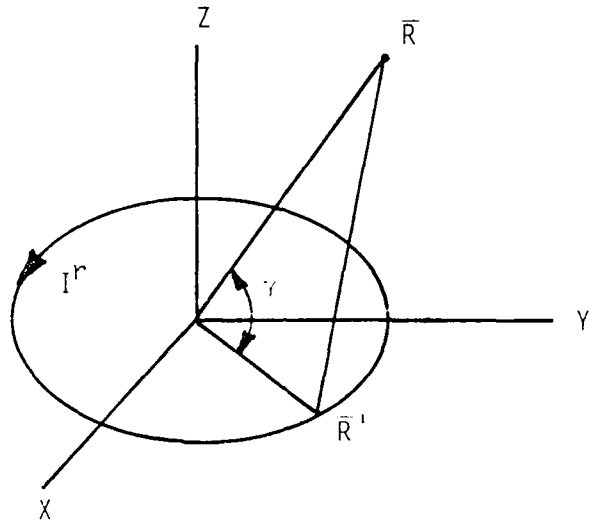


Figure 4.3 Geometry of a constant current circular loop antenna

functions the potential integral for $\bar{A}(\bar{R})$ is evaluated. For $R > a$ we have:

$$\bar{A}(\bar{R}) = \hat{z} \left(-\frac{j\mu_0 I_0 a}{4} \right) \times \sum_{n=0}^{\infty} \frac{(-1)^{n+1} (4n+3)(2n)!}{2^{2n} (n+1)(n!)^2} \times j_{2n+1}(ka) h_{2n+1}^{(2)}(kR) P_{2n+1}^1(\cos\theta) \quad (4.36)$$

Let us set:

$$|\bar{R} - \bar{R}'| = \sqrt{r^2 + r'^2 - 2rr' \cos\phi'} \quad (4.37)$$

with:

$$r^2 + r'^2 = R^2 + a^2$$

$$r \cdot r' = aR \sin\theta$$

comparing with:

$$|\bar{R} - \bar{R}'| = \sqrt{(R^2 + a^2 - 2aR \cos\gamma)}$$

where: $\cos\gamma = \sin\theta \cos\theta' \cos\phi$.

We conclude that γ is the angle between two position vectors \bar{r} and \bar{r}' with angular coordinates:

$$\theta = \frac{\pi}{2}, \quad \phi = 0 \quad \theta' = \frac{\pi}{2}, \quad \phi = \phi'$$

From (4.38) we have

$$|\bar{r}'| = \left\{ \frac{1}{2}(R^2 + a^2 \pm \sqrt{(R^2 + a^2)^2 - 4(aR \sin\theta)^2}) \right\}^{1/2}$$

$$|\bar{r}'| = (R^2 + a^2)^{1/2} \left\{ \frac{1}{2}(1 \pm \sqrt{1 - \kappa^2}) \right\}^{1/2}$$

$$\kappa = \frac{2aR \sin\theta}{R^2 + a^2} < 1 \quad (4.39)$$

Now we can use the addition theorem for the spherical Hankel function:

$$h_0^{(2)}(k|\bar{R} - \bar{R}'|) = h_0^{(2)}(k|\bar{r} - \bar{r}'|)$$

and the addition theorem for Legendre polynomials:

$$P_n(\cos\gamma) = P_n(\cos\theta)P_n(\cos\theta') + 2 \sum_{m=1}^n \frac{(n-m)!}{(n+m)!} P_n^m(\cos\theta) \times \\ \times P_n^m(\cos\theta') \cos m(\phi - \phi')$$

where $\cos\gamma = \cos\theta \cos\theta' + \sin\theta \sin\theta' \cos(\phi - \phi') = \cos\phi'$. Following analogous steps which led to (4.36) we obtain:

$$\bar{A}(\bar{r}) = \left(\frac{-j\mu k a I_0}{4} \right) \sum_{n=0}^{\infty} \frac{4n+3}{(n+1)(2n+1)} [P_{2n+1}^1(0)]^2 \times \\ \times j_{2n+1}(k r') h_{2n+1}^{(2)}(k r) \\ r' < r \quad (4.40')$$

Furthermore we have [7]:

$$P_{2n+1}^{\mu}(0) = \frac{\mu^{-1/2} e^{j\pi(\mu+\nu)} \Gamma(\frac{1}{2} + \frac{1}{2}\nu + \frac{1}{2}\mu)}{2^{\pi} \Gamma(1 + \frac{1}{2}\nu - \frac{1}{2}\mu)}$$

Therefore:

$$P_{2n+1}^1(0) = (-1)^{n+1} \frac{(2n+1)!}{2^{2n} (n!)^2}$$

Finally we have:

$$\begin{aligned} \bar{A}(\bar{R}) = & \hat{z} \left(-\frac{j\omega ka I_0}{4} \right) \sum_{n=0}^{\infty} \frac{(4n+3)(2n+1)}{n+1} \left[\frac{(2n)!}{2^{2n} (n!)^2} \right]^2 \times \\ & \times j_{2n+1}(k\nu') h_{2n+1}(k\nu) \quad \nu' < \nu \end{aligned} \quad (4.4)$$

Thus electric field intensity can be obtained as:

$$\begin{aligned} \bar{E}(\bar{R}) = & -j\omega \left(1 + \frac{1}{k^2} \nabla \cdot \nabla \right) \bar{A} = -j\omega \bar{A} = \\ = & \hat{z} \left(-\frac{(ka)^2 I_0}{4a} \right) \sum_{n=0}^{\infty} \frac{4n+3}{(n+1)(2n+1)} [P_{2n+1}^1(0)]^2 \times \\ & j_{2n+1}(k\nu') h_{2n+1}(k\nu) \quad \nu' < \nu \end{aligned} \quad (4.41)$$

Note that in obtaining the expression (4.41) we have used the following relation:

$$\nabla \cdot \bar{A} = \frac{1}{R_0} \frac{\partial}{\partial t} A_0 = 0.$$

Now we are in a position to obtain the mutual impedance of the antennas shown in Figure 4.2. Application of the reciprocity theorem to one of the two antennas, say antenna 2, yields [5.2].

$$V^r = -\frac{1}{I^t} \int_{V'} \bar{E}^i \cdot \bar{J}^t dv'$$

where

V^r \equiv open circuit voltage of antenna 2 in receiving mode

I^t \equiv current of antenna 2 in transmitting mode

\bar{E}^i \equiv incident electric field when antenna 2 is removed

$\vec{J}^t \equiv$ current density of antenna 2 in transmitting mode.

Noting that:

$$z_{21} = \frac{V_2}{I_1} \Big|_{I_2=0} = \frac{V_{2OC}}{I_1}$$

we can equivalently write:

$$z_{21} = - \frac{1}{I_1 I_2} \int_{V'} \vec{E}^i \cdot \vec{J}_2(\vec{R}') dv' \quad (4.42)$$

where:

$$\vec{J}_2(\vec{R}') = \hat{\phi}' I_2 \delta(\cos\theta\theta') \frac{\delta(R'-a)}{R'}$$

Using (4.41) in (4.42) we have:

$$\begin{aligned} z_{21} &= - \int_{V'} \left(- \frac{(ka)^2 \eta}{4a} \right) \sum_{n=0}^{\infty} \frac{4n+3}{(n+1)(2n+1)} [P_{2n+1}^1(0)]^2 \times \\ &\quad \times j_{2n+1}(k\nu') h_{2n+1}^{(2)}(k\nu) \delta(\cos\theta\theta') \frac{\delta(R'-a)}{R'} \times \\ &\quad \times R'^2 \sin\theta\theta' dR' d\theta' d\phi' \\ z_{21} &= \frac{(ka)^2 \eta}{4a} \sum_{n=0}^{\infty} \frac{4n+3}{(n+1)(2n+1)} [P_{2n+1}^1(0)]^2 \times \\ &\quad \times j_{2n+1}(k\nu') h_{2n+1}^{(2)}(k\nu) \int_{V'} \delta(\cos\theta\theta') \frac{\delta(R'-a)}{R'} R'^2 \sin\theta\theta' dR' d\theta' d\phi' \end{aligned}$$

we have:

$$\begin{aligned} z_{21} &= \eta \frac{2}{2} (ka)^2 \sum_{n=0}^{\infty} \frac{4n+3}{(n+1)(2n+1)} [P_{2n+1}^1(0)]^2 \times \\ &\quad j_{2n+1}(k\nu') h_{2n+1}^{(2)}(k\nu) \end{aligned} \quad (4.43)$$

For $|ka| \ll 1$ and $a \ll \rho$ we have:

$$\chi = \frac{2aR_0 \sin\theta_0}{R^2 + a^2} = \frac{2a^2}{\rho^2 + 2a^2} \ll 1 \quad (4.39')$$

$$\begin{aligned}
 \psi' &= (R^2 + a^2)^{1/2} \left\{ \frac{1}{2} [1 \pm \sqrt{1 - \nu^2}] \right\}^{1/2} \\
 &= (R^2 + a^2)^{1/2} \left\{ \frac{1}{2} [1 \pm (1 - \frac{1}{2} \nu^2 + O(\nu^4))] \right\}^{1/2} \\
 \psi' &= (R^2 + a^2)^{1/2} \frac{\nu}{2} [1 + O(\nu^2)] = \frac{a^2}{(c^2 + 2a^2)^{1/2}} [1 + O(\nu^2)] \quad (4.44) \\
 \psi &= (R^2 + a^2)^{1/2} [1 - \frac{1}{8} \nu^2 + O(\nu^4)] = (c^2 + 2a^2)^{1/2} [1 + O(\nu^2)].
 \end{aligned}$$

Therefore:

$$\begin{aligned}
 k_1' &= ka \frac{a}{(c^2 + 2a^2)^{1/2}} [1 + O(\nu^2)] = ka \frac{a}{(c^2 + 2a^2)^{1/2}} [1 + O(\frac{a^4}{4})] \\
 k_2' &= k(c^2 + 2a^2)^{1/2} [1 + O(\nu^2)] = k(c^2 + 2a^2)^{1/2} [1 + O(\frac{a^4}{4})] \quad (4.44')
 \end{aligned}$$

Let us note that [11]:

$$j_n(z) = \left(\frac{\pi}{2z}\right)^{1/2} J_{n+1/2}(z) = 2^n z^n \sum_{m=0}^{\infty} \frac{(-1)^m (n+m)!}{m! (2n+2m+1)!} z^{2m} .$$

The asymptotic expansion for $h_n^{(2)}(z)$ for large argument z reads:

$$\begin{aligned}
 h_n^{(2)}(z) &= \left(\frac{\pi}{2z}\right)^{1/2} H_{n+1/2}^{(2)}(z) = \frac{1}{2} e^{-j(z-(n+1)\frac{\pi}{2})} \left\{ \right. \\
 &\quad \left. \sum_{m=0}^{F-1} \frac{(-n)_m (n+1)_m}{m! (-2jz)^m} + O(z^{-D}) \right\} .
 \end{aligned}$$

We conclude from the above that under the conditions imposed on a and c the first term of the series (4.43) will be sufficient for computation of z_{21} :

$$\begin{aligned}
 z_{21} &= \frac{3\pi}{2} (ka)^2 (P_1^1(0))^2 j_1(k\nu') h_1^{(2)}(k\nu) + \\
 &\quad + O\left\{ (ka)^2 (k\nu')^3 (k\nu)^{-1} \right\} \\
 z_{21} &= \frac{3\pi}{2} (ka)^2 j_1(k\nu') h_1^{(2)}(k\nu) + O\left\{ \frac{(ka)^8}{(k\nu)^4} \right\} \quad (4.45)
 \end{aligned}$$

$$\begin{aligned}
 z_{21} &= -\eta \frac{\pi}{2} (ka)^2 \frac{v'}{v} e^{-jk\rho} + O\left\{\frac{(ka)^8}{(k\rho)^4}\right\} \\
 &= -\eta \frac{\pi}{2} (ka)^2 \frac{a^2}{\rho^2 + a^2} \exp\{-jk(\rho^2 + 2a^2)^{1/2}\} \\
 &\quad + O\left\{\frac{(ka)^8}{(k\rho)^4}\right\} \tag{4.46}
 \end{aligned}$$

Let us once more recall that the impedance which should be used in (3.1) can be obtained from (4.35) and (4.46) by means of:

$$z_{in} = z_{11} - z_{12} = z_{11} - z_{21}$$

and changing ρ to $2d$.

4.4 Input impedance of two antisymmetrically driven identical coplanar circular loop antennas.

The self impedance for this configuration of loops under assumptions imposed on the geometry of the antennas in section 3.1 is identical with the input impedance of a single loop antenna and can be obtained from (4.35). The mutual impedance can be obtained in exactly the same manner as followed in section 4.3, however the integrals appearing in this case are a little involved and for the purpose of the problem at hand it suffices to use an asymptotic formula for z_{12} which is developed in [10.2] based on effective heights of the transmitting antennas:

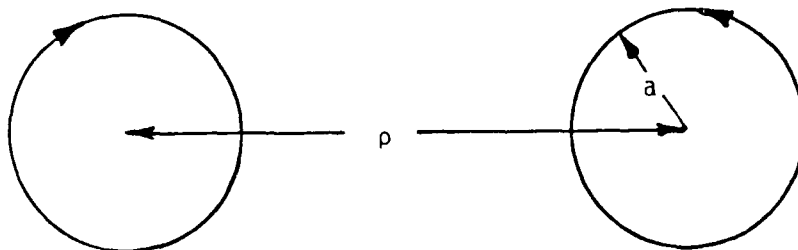


Figure 4.4 Coplanar loop antennas

$$\begin{aligned}
 z_{12} &= jn \frac{e^{-jkP}}{2\lambda P} (\bar{h}_1 \cdot \bar{h}_2) = jn \frac{e^{-jkP}}{2\lambda P} \times \\
 &\times \left[\frac{j}{k} (ka)^2 \sin^2 \theta_1 \right]_{\theta_1 = \frac{\pi}{2}} \times \left[\frac{j}{k} (ka)^2 \sin^2 \theta_2 \right]_{\theta_2 = \frac{\pi}{2}} (\hat{s}_2 \cdot \hat{s}_2) \\
 z_{12} &\approx -j \frac{\pi}{4} n(ka)^4 \frac{e^{-jkP}}{kP} \quad . \quad (4.47)
 \end{aligned}$$

5. Correlation of the unperturbed surface fields to the equivalent circuit parameters of the probes.

In previous sections an attempt was made to completely describe the equivalent circuit parameters of the different probes mounted on a corner reflector. Since any physical measurement performed by the probes can be described completely in terms of the open circuit voltage and the input impedance of the sensors, we will attempt to relate the surface field quantities in the absence of the sensors to the equivalent circuit parameters of the sensors, or in other words to the measurable quantities.

In section 2 it was shown that for a plane wave illumination of the wedge with electric field polarized perpendicular to the wedge axis surface current and charge densities are respectively given by:

$$\bar{K}(\bar{R}) = -x 4H_0^i \sin \theta \sin \theta \sin(kx \sin \theta) \quad x > 0 \quad z=0 \quad (2.3)$$

$$\sigma(\bar{R}) = j 4 E_0^i \sin \theta \sin \theta \sin(kx \sin \theta) \quad x > 0 \quad z=0 \quad (2.5)$$

On the other hand the open circuit voltage of a short monopole mounted on the wedge was found to be:

$$V_{OC}^r = j2\lambda E_0^i \sin \theta \sin \theta \sin(kx \sin \theta). \quad (3.3)$$

Comparing (2.5) with (3.3) we establish that:

$$\sigma = \frac{2}{\lambda} V_{OC}^r \quad (5.1)$$

The unperturbed surface charge density is therefore related to the open circuit voltage of the probe by an equivalent capacitance per unit area:

$$c_{eq} \triangleq \frac{2\epsilon}{\lambda} \quad \text{Farad/m}^2 \quad (5.2)$$

Equation (5.1) is the manifestation of the electric coupling of the monopole probes and further justifies the name of 'charge probes' given to this kind of sensors.

Similarly the V_{oc}^r for a semiloop whose axis is parallel to the wedge axis was found to be:

$$V_{oc}^r = -j2\omega(\mu\pi a^2)H_0^i \cos(kx) \sin\theta \quad (3.4)$$

Comparing (3.4) with (2.3) we have:

$$V_{oc}^r = j\omega \frac{\mu\pi a^2}{2} k_x \quad (5.3)$$

That is the equivalent inductance relating V_{oc}^r to unperturbed current density is given by:

$$L_{eq} = \frac{1}{2} \mu(\pi a^2) \quad \text{Henry m.} \quad (5.4)$$

It is obvious that the coupling of the probe to the electromagnetic field in this case is of magnetic type. Let us finally note that for the plane wave whose electric field is polarized parallel to the wedge axis the surface currents and the corresponding surface magnetic field can be detected by a semiloop sensor whose plane is parallel to the current lines. From (2.7) and (3.5) we obtain for this case:

$$V_{oc}^r = j\omega \frac{\mu\pi a^2}{2} k_y \quad (5.5)$$

That is to say the equivalent inductance for this case is also given by (5.4).

Let us conclude from the above results that as long as our sensors are electrically small low frequency elements relating the open circuit voltage of the probes to the surface fields only depend on the geometrical characteristics of the probes and are independent of the characteristics of the source.

References

1. Collin, R. E. and Zucker, F. J., Antenna Theory Part I, McGraw-hill Book Company, New York, 1969, Chap. 11.
2. Dyson, J. D., IEEE Trans. AP., VOL. AP21, July 1973, p. 446.
3. Green, F. M., J. Res. Nat. Bur. Stand., Sec. 3, Vol. 71C, Oct. - Dec. 1967, p. 319.
4. Huerta, M. A. and Gonzalez, G., J. Appl. Phys., Vol. 43, No. 10, Oct. 1972, p. 3975.
- 5.1 Jordan, E. C. and Balmain, K. G., Electromagnetic Waves and Radiating Systems, second edition, Prentice-Hall, N.J. 1968, p. 335.
- 5.2 ----- p. 435.
6. King, R.W.P. and Chang, V.W.H., IEEE Trans. AP., Vol. AP16, May 1968, p. 309.
7. Magnus, W., Oberhettinger, F. and Soni, R. P., Formulas and Theorems for the Special Functions of Mathematical Physics, third edition, Springer-Verlag, New York, 1966, p. 171.
8. Martin, Jr., E.J., Proc. IEEE, Vol. 51, July 1963, p. 1042.
- 9.1 Ramo, S., Whinnery, J. R. and Van Duzer, T., Fields and Waves in Communication Electronics, John Wiley, New York, 1965, p. 309.
- 9.2 ----- p. 656.
- 10.1 Tai, C.T., Technical Report No. 32, Project No. 591, Stanford Research Institute, Stanford, California, Dec. 1952.
- 10.2 ----- Antenna Theory Notes, Department of Electrical and Computer Engineering, The University of Michigan, Ann Arbor, Michigan.
11. Watson, G. N., Theory of Bessel Functions, second edition, Cambridge University Press, London, 1952, p. 40 and 198.